agronomy

MDPI

Article

Variations in Growth, Physiology, and Antioxidative Defense Responses of Two Tomato (*Solanum lycopersicum* L.) Cultivars after Co-Infection of *Fusarium oxysporum* and *Meloidogyne incognita*

Ambreen Maqsood [1,2], Haiyan Wu [1,*], Muhammad Kamran [3], Hussain Altaf [1], Adnan Mustafa [4], Sunny Ahmar [5], Nguyen Thi Thang Hong [1], Kinza Tariq [1], Qiong He [1] and Jen-Tsung Chen [6]

1 Guangxi Key Laboratory of Agric-Environment and Agric-products Safety, Agricultural College of Guangxi University, Nanning 530004, Guangxi, China; ambreenagrarian@gmail.com (A.M.); altafhussain2k16@outlook.com (H.A.); nguyenthanhhong82@gmail.com (N.T.T.H.); kinzatariq322@gmail.com (K.T.); Heqiong3344@163.com (Q.H.)
2 Department of Plant Pathology, University College of Agriculture and Environmental Sciences, The Islamia University of Bahawalpur, Bahawalpur 63100, Pakistan
3 Key Laboratory of Arable Land Conservation (Middle and Lower Reaches of Yangtze River), College of Resources and Environment, Ministry of Agriculture, Huazhong Agricultural University, Wuhan 430070, Hubei, China; kamiagrarian763@gmail.com
4 National Engineering Laboratory for Improving Quality of Arable Land, Institute of Agricultural Resources and Regional Planning, Chinese Academy of Agricultural Sciences, Beijing 100081, China; adnanmustafa780@gmail.com
5 National Key Laboratory of Crop Improvement Genetics, College of Plant Sciences and Technology, Huazhong Agricultural University, Wuhan 430070, Hubei, China; sunny.ahmar@yahoo.com
6 Department of Life Sciences, National University of Kaohsiung, Kaohsiung 811, Taiwan; jentsung@nuk.edu.tw
* Correspondence: whyzxb@gmail.com; Tel.: +86-771-3235-612

Received: 16 November 2019; Accepted: 14 January 2020; Published: 22 January 2020

Abstract: The soil-borne fungus *Fusarium oxysporum* (*Fo*) and the nematode *Meloidogyne incognita* (*Mi*) are destructive pathogens that cause substantial yield losses to tomato (*Solanum lycopersicum* L.) crops worldwide. The present study sought to elucidate the physiological, biochemical, and cytological responses of tomato cultivars (Gailing maofen 802 and Zhongza 09) by root invasion of *Fo* (1×10^5 CFUmL^{-1}) and *Mi* (1500 second-stage juveniles (J2) alone and in combination after 14 days. Results revealed that combined inoculation of *Fo* and *Mi* significantly increased disease intensity, electrolyte leakage, and hydrogen peroxide and malondialdehyde contents; and decreased photosynthetic capacity and enzyme activity in both cultivars as compared to their solo inoculation. Increasing the disease intensity reduced the maximum morphological traits, such as shoot length, total dry weight, and total chlorophyll contents, in G. maofen 802 (by 32%, 54.2%, and 52.3%, respectively) and Zhongza 09 (by 18%, 32%, and 21%, respectively) as compared to the control. Others factors were also reduced in G. maofen 802 and Zhongza 09, such as photosynthetic capacity (by 70% and 57%, respectively), stomatal conductance (by 86% and 70%, respectively), photochemical quantum yield of photosystem II (YII) (by 36.6% and 29%, respectively), and electron transport rate (by 17.7% and 10%, respectively), after combined inoculation of *Fo* and *Mi*. Furthermore, the combined infestation of *Fo* and *Mi* resulted in reduced activity of plant-defense-related antioxidants in G. maofen 802 compared with their single application or control. However, these antioxidants were highly up-regulated in Zhongza 09 (by 59%–93%), revealing the induction of tolerance against studied pathogens. The transmission electron microscopy (TEM) results further demonstrated that root cells of Zhongza 09 had unique tetrahedral crystal-like structures in the membrane close to mitochondria under all

treatments except control. Therefore, it is concluded that *Mi* caused severe root damage, suppressed plant growth, depleted antioxidants, and caused high generation of ROS in the presence of *Fo* as compared to its solo inoculation. Tolerant cultivars adopted different mechanistic strategies at the structural and cellular levels to tolerate the *Mi* and *Fo* stresses.

Keywords: *Solanum lycopersicum*; *Meloidogyne incognita*; *Fusarium oxysporum*; disease intensity; photosynthetic traits; antioxidants; cytology

1. Introduction

Continuous cropping is a common practice in intensive agricultural production, particularly for horticultural crops. However, continuous cropping can negatively affect soil fertility, physicochemical properties, and microbial communities, leading to a decline in crop productivity [1]. Changes in microorganism populations in soils are critical to the sustainability of soil-based ecosystem functions [2]. Soil-borne pathogens and nematode infestations cause significant yield losses and lower the quality of horticultural crops worldwide [3]. Among the most familiar soil-borne diseases, Fusarium wilt is particularly challenging because of its complexity and long survival time in soil [4]. In addition, as the soil environment is complex, this makes it difficult to detect, diagnose, and control diseases in a timely manner [5]. The *Fusarium* species exhibit wide-ranging ecological functions, for example as saprophytes, endophytes, and plant and animal pathogens [6]. By virtue of their morphology, host interactions, and molecular characterization, it is reported that the genus *Fusarium* consists of about 200 species in 22 constituent species complexes [7], which are considered to be the most destructive pathogenic plant fungi [6]. Within the genus Fusarium, *Fusarium oxysporum* (*Fo*) specifically contains the major fungal phytopathogens [8]. It has been well-established that *Fusarium oxysporum* is engaged in tomato crown and root rot diseases, causing remarkable losses in tomato fruit in both field and greenhouse cultivation [9].

After introduction into a host plant, *Fusarium oxysporum* clogs the xylem vessels with mycelium, spores, or polysaccharides, causing wilting in tomato [10]. Moreover, the perpetual nuclear cell division in vascular bundles causes tylosis [11], thus blocking the transportation of water and nutrients to the aerial part of the plant. Aerial symptoms of Fusarium wilt start with the chlorosis and wilting of older leaves and progress towards the apex, eventually causing plant death.

Similarly, among the diverse groups of biotic agents that cause soil-borne diseases, plant-parasitic nematodes are the most damaging roundworms, classified as: (i) ectoparasites, in which the nematode remains outside of the plant and uses its stylet to feed from the plant root cells; (ii) semi-endoparasites, in which nematodes partially penetrate the plant and feed at some point during their life cycle; (iii) migratory endoparasites, in which nematodes spend much of their time migrating through root tissues, destructively feeding on plant cells; and (iv) sedentary endoparasites, in which the nematode spends the majority of its lifespan sedentary inside the plant tissue, establishing a highly specialized parasitism [12]. *Meloidogyne incognita* is a species of root knot nematode (RKN) that is endoparasitic and is well known for causing damage to a broad range of horticultural and field crops [6]. At the onset of RKN invasion, the second-stage juveniles of *Meloidogyne* spp. enter into the root vascular tissues through the elongation zone and move into the root apex through the cortex [13], establishing a permanent feeding site. where they complete their lifecycle without killing the cells around them. Once feeding sites are established, RKN stimulates cells to create a specialized structure composed of multinucleate and hypertrophied giant cells, which result from the redifferentiation of vascular root cells [14]. The continuous feeding process of RKN damages the plant's root system and reduces the plant's ability to absorb water and nutrients, providing an opportunity for other plant pathogens to invade the root, thus further weakening the plant [15]. Previously, it has been reported that *Meloidogyne* spp. causes severe infection in tomato when followed by *Fusarium oxysporum* infestation [16–18]. It

induces changes in developmental and morphological attributes of crops, in addition to systemic symptoms such as wilting, dwarfing, yellowing, and susceptibility to other pathogens [19].

After pathogenic infestation, a variety of local and systemic plant responses are stimulated. In the protective defense mechanism, the first steps are local remodeling of the cell wall constituents, deposition of callose next to the infected cells, and then production of pathogenesis-related (PR) proteins following the addition of reactive oxygen species (ROS) in leaves in response to pathogens [20]. Also, numerous biochemical processes linked to membrane permeability shifts, oxidative-destruction of biopolymers, malfunctioning of mitochondrial activity, and reticence of respiration have been observed at the sub-cellular level [21]. The ROS generation interrupts the normal redox environment of the plant cell, particularly near the invaded cells and in the cell walls close to hypersensitive response cells. To compensate for the ROS caused by pathogens, a resistant host plant preferably generates a higher amount of photosynthetic pigments (such as chlorophyll) and biochemical contents (total proteins and antioxidants enzymes) than susceptible host plants [22], hence surviving under unfavorable conditions.

Considering the adverse effects imposed by soil-borne plant diseases, it is imperative to develop strategies in order to control and eliminate their occurrence and intensity for sustainable agricultural production. In this regard, management of soil-borne diseases through genetic resistance in hosts can offer a long-term and economical control strategy for Fusarium wilt in tomato, and many commercial hybrid resistant cultivars have been developed in recent years. However, the effectiveness of resistant cultivars is diminished by the co-infection of fungi and plant-parasitic nematodes [23]. The few studies to date on the subject have reported on nematode–pathogen relationships and their effects on growth and physiological traits of tomato. In addition, the cytological responses of tomato roots against co-infection remains relatively neglected. Therefore, the present study was carried out to investigate the influence of *Meloidogyne incognita* (*Mi*) on disease severity in the presence of *Fo* on two tomato cultivars. The specific objectives of this study were to evaluate the relative physiological, biochemical, and root cytological responses of two commercial hybrid cultivars of tomato, namely Gailing maofen 802 and Zhongza 09, against two soil-borne pathogens, *Meloidogyne incognita* (*Mi*) and *Fusarium oxysporum* (*Fo*), when applied individually and in combination. Both varieties used in this experiment were susceptible to *Mi* and resistant to *Fo*.

2. Materials and Methods

2.1. Isolation of Fungal and Nematode Culture

Fusarium oxysporum (*Fo*) (accession number MN240928) used in this study was isolated from roots of vascular wilt-infected tomato in Tianyang County, Baise City, Guangxi Province, China. The strain was identified and confirmed using a polyphasic approach, involving morphological, biological, and genetic (amplification of fungal RNA using internal transcribed spacer (ITS) primer) methods [24]. DNA was extracted by cetyl trimethylammonium bromide (CTAB) method (Supplementary Materials, Protocol for DNA extraction of *Fusarium oxysporum*). For confirmation, the pathogenicity test was also performed on tomato seedlings according to suggestions made by Koch [25]. The fungal chlamydospores were obtained from 7-day-old potato dextrose agar (PDA) plates by abrading and cleaning of the culture with an autoclaved distilled water. Counting of conidia was done with the help of the hemocytometer chamber (Yancheng Cordial Medlab.Co., Ltd Jiangsu, China) under the stereomicroscope, fixed to constant number of 1×10^5 CFU mL^{-1}, and further used for bioassay for 35 days.

The root-knot nematode *Meloidogyne incognita (Mi*) was cultured in the nematology laboratory of Guangxi University, Nanning, China, via parenting on tomato roots from a single egg mass. After 35 days, egg masses were detached from infected tomato roots using sodium hypochlorite solution (NaOCl) (Chengdu Jinshan Chemical Reagent Co., Ltd. Chengdu, China) [26], allowed to hatch in Petri plates filled with sterilized water, and incubated at 27 °C for 3 days. The newly hatched second-stage juveniles (J2) were collected and used in this experiment.

2.2. Screening of Tomato Cultivars

An initial screening of different tomato cultivars collected from the Chinese Academy of Agriculture Sciences, Vegetable Seed Technology Co., Ltd., Beijing, China, was carried out against *Fo* and *Mi* (Supplementary Table S1). Among them, two desired tomato F1 commercial hybrid lines, namely Gailing maofen 802 (moderately resistant to Fusarium wilt and susceptible to *Mi*) and Zhongza 09 (highly resistant against Fusarium wilt and susceptible to *Mi*) were selected for this experiment (Supplementary Table S2).

2.3. Experimental Design and Treatment Plan

The experiment was conducted from November 2018 to January 2019 using a completely randomized design in the greenhouse of Guangxi University, China. Prior to sowing, tomato seeds of both varieties were surface sterilized in petri dishes (1.0% NaOCl for 15 min) and sown in MC6 plastic plant cell trays containing autoclaved peat moss. In addition, a total of 240 pots (21 cm diameter, 15 cm height) were prepared by adding 1 kg of autoclaved peat soil purchased from Nanning Guiyuxin Agricultural Technology Co., Ltd. [27]. Each treatment consisted of 40 replicates. Thirty-day-old non-infected tomato seedlings of uniform length and density were transplanted into these pots at 27 °C temperature and 50%–70% relative moisture content in a greenhouse. The experiment consisted of four treatments: (1) CK (non-inoculated plants); (2) *Mi* (plants inoculated with *Meloidogyne incognita*); (3) *Fo* (plants inoculated with *Fusarium oxysporum*; and (4) *Fo* + *Mi* (plants co-inoculated with *Fusarium oxysporum* and *Meloidogyne incognita*). Three holes were made around the rhizospheric zone of each plant and 1500 second-stage juveniles (J2) of *Mi* and 1×10^5 CFU mL^{-1} chlamydospores of *Fo* were added into either *Mi* alone, *Fo* alone, or co-treatment (*Fo* + *Mi*), respectively. All plants were irrigated with good quality water (sodium adsorption rate (SAR) = 12 meq/L, residual sodium carbonate (RSC) = 1.5 meq/L, electrical conductivity (EC) = 400 micromhos/cm at 25 °C, total dissolved solid = 300 mg/L) in equal amounts at the same intervals throughout the experiment. Observations were conducted to determine the percentage of plants showing chlorotic symptoms at 14 days after inoculation (DAI), while *Mi* population density per plant was evaluated at 35 DAI.

Moreover, a sequential application trial for *Fo* and *Mi* was also performed to check the disease intensity and nematode multiplication, organized into two groups: $Fo \xrightarrow{\text{After7days}} Mi$ (plants sequential inoculated with *Fusarium oxysporum* 7 days prior to *Meloidogyne incognita*) and $Mi \xrightarrow{\text{After7days}} Fo$ (plants sequential inoculated with *Meloidogyne incognita* 7 days prior to *Fusarium oxysporum*). All experiments were conducted twice under similar conditions and similar results were found.

2.4. Scoring of Chlorotic or Necrotic Symptoms and Disease Intensity

Each plant was assessed for standard disease assessment at 14 days after inoculation (DAI) (foliage) following the disease score (0–4) for *Fusarium oxysporum* (*Fo*): 0 = asymptomatic (healthy plants); 1 = up to 25% of leaves were chlorotic and wilted; 2 = up to 50% leaves were chlorotic and wilted; 3 = up to 75% of leaves chlorotic and wilted; 4 = 100% of the plant chlorotic or wilted. The disease austerity was observed from 0 days. The disease severity index was calculated by following the formula given by [28]:

$$DI\ (\%) = \frac{(Number\ of\ plants\ with\ ith\ score) \times (Value\ of\ ith\ score)}{(Total\ number\ of\ plants) \times (Highest\ value\ to\ symptoms)} \times 100$$

Three infected chlorotic plants from each treatment were randomly selected for *Fo* isolation. Small sections of the lower stem (2 × 3 × 8 mm) were surface-sterilized with 1.0% NaOCl for 1 min, rinsed with distilled and sterilized water twice, and placed in potato dextrose agar (PDA) medium for one week. Emerging fungal colonies were purified and identified morphologically and molecularly to confirm the presence of *Fo*.

2.5. Disease Assessment of Root Galls

After 35 days of the experiment, plant roots were stained to calculate *Mi* populations in the roots (number of females, number of eggs) and in the soil (number of second-stage juveniles) using a galling index, as previously described in [6]. For staining, tomato roots were washed carefully with tap water and then placed into the 0.5% NaOCl solution for 3–4 min by stirring the roots continuously with a spatula. Afterwards, the roots were rinsed again under running tap water. The roots were then heat-treated at 80 °C for 2 min in a beaker containing an acid fuchsin solution (0.35 g of acid fuchsin, 25 mL of acetic acid, and 75 mL of distilled water) [29]. Then, the roots were allowed to cool down, taken out of the solution, and washed again with tap water. Next, roots were treated with acidified glycerin and examined carefully under a microscope (OLYMPUS SZX2-ILLT, Tokyo Japan) to count the number of females, number of eggs, and the size of the galls. The second-stage juvenile (J2) population was assessed in soil by centrifugation and floating method [30], and juveniles were counted and expressed as J2 per 250 cm^3 of soil.

2.6. Assessment of Antioxidant Activities in Roots and Leaves of Tomato

The antioxidant enzyme (superoxide dismutase (SOD), catalase (CAT), polyphenol oxidase (PPO), ascorbate peroxidase (APX), and ascorbate oxidase (AAO)) activities of roots and leaves were estimated on the 14th day of inoculation with 4 repetitions. Fresh roots and leaves (0.1 g) were powdered in liquid nitrogen and suspended in 0.9 mL of 10 mM chilled phosphate-buffered solution (PBS) with a pH of 7.4. All procedures were carried out in a pre-chilled ice bath. Furthermore, the homogenate was centrifuged at 4 °C and 10,000 rpm for 10 min, and the resulting supernatant was collected for determination of antioxidant activities by using commercial assay kits purchased from Nanjing Jiancheng Bioengineering Co., Ltd. (Nanjing, China). For all enzyme activities, the absorbance was recorded on a microplate reader (Multiscan GO 1510, Thermo Fisher Scientific Oy, Ratastie, Finland).

The superoxide dismutase SOD (EC 1.15.1.1) activity was determined through a commercial kit Nanjing Jiancheng Bioengineering Co., Ltd. (Nanjing, China) by using the xanthine oxidase method and expressed in μ mg^{-1} protein [31]. The reaction mixture contained 50 mM sodium phosphate buffer (pH 7.6), 0.1 mM EDTA, 50 mM sodium carbonate, 12 mM L-methionine, 50 μM nitroblue tetrazolium (NBT), 10 μM riboflavin, and 100 μL of crude extract at a final volume of 3.0 mL. A control reaction was performed without crude extract. The SOD reaction was carried out by exposing the reaction mixture to white light for 15 min at room temperature. After 15 min, the reading was recorded at the absorbance of 550 nm on a microplate reader [32]. The catalase (CAT) (EC 1.11.1.6) activity was estimated based on the reduction of hydrogen peroxide (H_2O_2), which was diminished by ammonium molybdate to form a yellow complex, with absorbance noted at 405 nm. The reaction mixture contained 100 mM sodium phosphate buffer (pH 7.0), 30 mM H_2O_2, and 100 μL of crude extract at a total volume of 3.0 mL, and the reading was recorded on a microplate reader [33]. The polyphenols oxidase (PPO) (1.14.18.1) was catalyzed by the increase of the phenol substrate via characteristic light absorption at 420 nm for 30 s at 3 min intervals. The assay was performed with 100 mM sodium phosphate buffer (pH 7.0), 5 mM 4-methylcatechol, and 500 μL of crude extract at room temperature. The total volume of reaction mixture was 3.0 mL. One unit (U) of enzyme activity was defined as the amount of the enzyme that caused a change of 0.001 optical density (OD) value in absorbance per min [34]. Ascorbate oxidase (AAO) activity was measured by calorimetrically measuring the oxidized amount of ascorbate (AsA) at 265 nm absorbance for 10 s at 130 s intervals. The leaves and roots (approximately 50 mg) were homogenized with 0.1 m sodium phosphate at pH 5.6, 0.5 mm ethylene diamine tetraacetic acid (EDTA), 1 m NaCl, and 100 mL of spun extract, which was assayed rapidly at 265 nm at a final volume of 1 mL, containing 0.1 mm ascorbate in the same phosphate buffer. The absorbance decrease at 265 nm was followed by addition of the extract. The ascorbate peroxidase (APX) (EC 1.11.1.11) activity was measured by observing the oxidation of ascorbate with hydrogen peroxide, and absorbance was recorded at 290 nm for 10 s and at 10 s intervals. The reaction mixture contained 1.66 mL of 0.5 mmol/L ascorbate in phosphate buffer (pH 7.0) and 0.26 ml of 2 mmol/L H_2O_2 (both of which were freshly

prepared), along with 0.8 ml of enzyme extract. One unit of APX activity was defined as 1 mg of tissue protein catalyzed by 1 µmol ascorbate for 1 min [32]. The total soluble protein content was assessed following instructions according to the kit from Nanjing Jiancheng Bioengineering Institute Co., Ltd. (NJJBI), Nannjing, China. In total, 1 g of roots and leaves for each treatment was crushed in liquid nitrogen in a pre-cooled mortar and pestle. Then, 100 g 0.05 M tris buffer was added along with 300 mg fresh mass mL^{-1} buffer for extraction of protein. Additionally, 0.05 g of polypyrollidone (PVPP) was added to each sample during the homogenization. Afterward, the homogenate was centrifuged at 14,000 rpm for 20 min at 4 °C. Total protein contents were expressed as mg g^{-1} FW (fresh weight) [35].

2.7. Determination of Oxidative Stress Indicators

The hydrogen peroxide (H_2O_2) contents were measured according to the protocol mentioned on the Nanjing Jiancheng Bioengineering Co., Ltd. (NJJBI) kit (Nanjing, China) [35]. The 100 mg sample was ground in 1.0 mL of 0.1% (w/v) trichloroacetic acid (TCA) and centrifuged at 10,000 rpm for 30 min at 4 °C. The reaction mixture consisted of 0.5 mL of 0.1 M potassium phosphate buffer and 2 mL of 1 M KI reagent. The reaction was allowed to develop for 1 h in the dark, and the concentration of H_2O_2 in samples was recorded at 410 nm using a microplate reader (Multiscan GO 1510, Finland) and expressed as µmol g^{-1} FW. Malondialdehyde (MDA) contents were determined by the chemical reaction of malondialdehyde with trichloroacetic acid (TCA) by thiobarbituric acid (TBA) method [35]. The homogenate was centrifuged at 10,000 rpm for 20 min with 3 mL of 0.5% (v/v) TBA in 20% TCA. The mixture was incubated in a water bath for 30 min and then quickly cooled in an ice bath. Then, the samples were again centrifuged at 10,000 rpm for 5 min. The absorbance was measured at 532 and 600 nm in a microplate reader (Multiscan GO 1510, Thermo Fisher Scientific Oy, Ratastie, Finland), according to the instructions in the commercial assay kit.

2.8. Plant Biomass Accumulation

For analysis of growth parameters, plants were carefully harvested at 14 DAI, showing complete expression of chlorotic disease symptoms. Leaves and roots were carefully washed, air-dried, and plant fresh weight (g) and height (cm) were measured. The fresh biomass of shoots and roots were calculated using a digital balance with 0.0001 g accuracy. The roots were examined using Delta-T Scan (Delta-T Devices, Ltd. Cambridge, UK) and winRHIZO (Regent Instruments, Inc. Qubec, Canada) root scanner systems to measure area, density, and diameter [36]. Afterwards, plant tissues were oven dried (Memmert, Beschickung loading, Model 100–800, Schwabach, Germany) at 67 °C until they reached a constant weight to determine dry biomass [37].

2.9. Total Chlorophyll Contents

Total Chlorophyll contents were extracted according to the protocol given in [38]. Briefly, 0.1 g fresh leaf tissue was ground in the autoclaved mortar and pestle with 10 ml of 80% acetone. The supernatant was extracted in Eppendorf tubes and stored in the dark for 24 h. The UV-visible spectrophotometer (Multiscan GO 1510, Thermo Fisher Scientific Oy, Ratastie, Finland) was used to measure the concentrations of chlorophyll at 645 nm and 663 nm, respectively, and the readings were taken within 90 min to avoid acetone volatilization. The concentration of total chlorophyll was calculated according to the formulae given by [39] and expressed as mg g^{-1} FW (fresh weight).

2.10. Proline Contents

Here, 0.1 g fresh leaves were homogenized in quartz sand and 6 mL of 3% sulfosalicylic acid was centrifuged at 8000 rpm at 25 °C for 5 min. The supernatant was reacted with 1000 µL acetic acid and 1500 µL ninhydrin solution. The mixture was heated for 1 h at 100 °C. After this, the reaction was further accelerated by adding 2500 µL toluene and vertexing the solution for 30 seconds. Measurement of the absorption of chromophore was taken at 520 nm [40].

2.11. Electrolyte Leakage

Electrolyte leakage (EL) was analyzed through the method given by [41]. For this purpose, 0.1 g leaf tissue was cut into small pieces, placed in a tube containing 10 mL deionized water, and kept in a water bath for 2 h at 32 °C. The value of initial conductance (E1) of the bathing solution after incubation was measured using an electrical conductivity meter (Shangai Yoke Instrument Co., Ltd. Shangai, China). The leaves samples were autoclaved at 121 °C for 20 min to release all the electrolytes. The samples were cooled to 25 °C to measure the final conductance (E2). The final electrolyte leakage was calculated by the following formula:

$$EL\ (\%) = \frac{E1}{E2} \times 100$$

2.12. Leaf Gas Exchange and Fluorescence Analysis

A portable gas exchange fluorescence system (GFS-3000; Heinz Walz, Effeltrich, Germany) was used to measure gas exchange attributes, including intracellular CO_2 concentration (Ci), transpiration rate (Tr), stomatal conductance (gs), and net photosynthesis (Pn) between 08:30 and 10:30. The average leaf temperature, photosynthetically active radiation (PAR), flow rate, and CO_2 concentration were estimated at 28 ± 0.8 °C, 1000 ± 14 µmol m^{-2} s^{-1}, 0.5 µmol s^{-1}, and 350 ± 3 µmol CO_2 mol^{-1}, respectively. The readings were taken from 3 consecutive fully expanded leaves per plant from at least five different places. Measurements of the net rate of chlorophyll fluorescence were performed with a leaf clip holder using a convenient, portable saturation pulse fluorimeter (PAM-2100, 2030-B; Walz, Effeltrich, Germany). Measurements of the *Fo* minimal level of fluorescence and Fm maximal level of fluorescence of darkness-adjusted leaves were made between 07:00 and 08:00. Readings for *Fo* were taken at a frequency of 0.6 kHz with a 0.5 µmol measurement light. For Fm, the saturating pulse was recorded at > 8000 µmol m^{-2} s^{-1} for 0.8 s. Fv was determined as the variable fluorescence (Fv − Fm = *Fo*). On the other hand, the possible potential quantum yield of PSII (Fv/Fm) was also estimated. Finally, the following parameters were obtained: the effective PSII quantum yield (YII), the photosynthetic electron transport rate (ETR), the non-photochemical quenching (qN), and potential quantum yield of PSII (Fv/Fm).

2.13. Transmission Electron Microscopy

Tomato roots were prepared for transmission electron microscopy (TEM) at 14 DAI according to Balestrini et al. [42]. Briefly, 0.5 cm root segments were obtained using an EM UC7 ultramicrotome (Leica, Wetzlar, Germany) with a Daitome Ultra 45° diamond knife. The samples were fixed in 2.5% (v/v) glutaraldehyde phosphate buffer (0.5 mM pH 7.4), followed by 1% (*w*/*v*) osmium tetroxide, and dehydrated in ethanol series (30%, 50%, 70%, 90%, 100%) at room temperature. Sectioned samples were then stained with uranyl acetate and lead citrate using carbon–copper mesh. Root sections were observed using a HT7700 transmission electron microscope (Hitachi, Tokyo, Japan) operating at 80.0 kV accelerating voltage.

2.14. Statistical Analyses

Data were analyzed using factorial analysis of variance (ANOVA), with treatments and cultivars as the two predictor variables. The data presented were the mean of three replications. The significant differences among treatment means were analyzed using Tukey's test at $p \leq 0.05$ using statistical software SPSS 16.0. (IBM, Madison, NY, USA). Graphical representation was done on Origin Pro 9.1 (Origin Lab Corporation, Northampton, MA, USA).

3. Results

3.1. Disease Assessment

The disease intensity (DI) results showed that both varieties of tomato were significantly affected by the co-inoculation of *Fo* and *Mi* at 14 DAI. The maximum (100%) disease intensity with chlorotic leaves was observed in tomato variety G. maofen 802 by applying combined inoculum (*Fo* + *Mi*) at 14 DAI (Supplementary Figure S1). In contrast, in Zhongza 09, 8.5% disease intensity was noticed, with few chlorotic leaves present. The sequential smears of *Fo*→*Mi* and *Mi*→*Fo* after 7 days also showed 85.4% and 95.1% disease intensity, respectively (Table 1). The serial application of *Mi*→*Fo* showed higher disease intensity percentage than concurrent *Fo* + *Mi* infestation. *Mi* and *Fo* solo applications on both varieties did not show any foliar symptoms at 14 days.

Table 1. Disease intensity on two tomato cultivars (G. maofen 802 and Zhongza 09) under greenhouse conditions at 14 days after inoculation (DAI).

Treatments	Disease Intensity (%)	
	G. maofen 802	Zhongza 09
Control	0.0	0.0
Meloidogyne incognita (*Mi*)	0.0	0.0
Fusarium oxysporum (*Fo*)	0.0	0.0
Meloidogyne incognita + *Fusarium oxysporum*	100	8.5
Fusarium oxysporum $\xrightarrow{\text{After7days}}$ *Meloidogyne incognita*	85.4	3.1
Meloidogyne incognita $\xrightarrow{\text{After7days}}$ *Fusarium oxysporum*	95.1	7.6

3.2. Interactive Effects of Fo and Mi on Biomass Accumulation

Fo and *Mi* interactive infestation as well as their single forms significantly reduced biomass of both cultivars of tomato as compared to control. The combined inoculation of *Mi* and *Fo* remarkably affected the plant growth, and significantly decreased the shoot length by 32%, total fresh biomass by 54.1%, and total dry biomass by 54.2% as compared to control in G. maofen 802. In addition, *Mi* inoculum moderately reduced the shoot length by 22% and total dry biomass by 28%, while total fresh weight was increased by 12% as compared to control at 14 DAI. For the Zhongza 09 variety, co-inoculation of *Fo* and *Mi* reduced the plant height by 18%, total dry mass by 32%, and total fresh weight by 19% compared with untreated plants, while plants treated with *Mi* or *Fo* alone remained similar to control (Figure 1A–C). The root morphologies of both varieties were significantly affected by combined inoculation of *Fo* and *Mi*. The maximum reductions in root surface area (62%) and root length density (62.2%) were shown in G. maofen 802 variety under *Fo* and *Mi* combined treatment (Figure 1E,F). Contrarily, a root surface area reduction of 27.5% was noted after *Mi* infestation in G. maofen 802 as compared to control. In Zhongza 09, *Fo* and *Mi* co-inoculation significantly reduced the root surface area by 29% and root length density by 39%, which was higher than the single treatment of *Fo* and *Mi*. Under *Fo* treatment, both varieties showed minute differences in all traits at 14 DAI.

3.3. Interactive Effect of Fo and Mi on Chlorophyll Contents

The results revealed that significant ($p \leq 0.05$) reductions in total chlorophyll contents were observed in the leaves of both varieties under single inoculation and co-inoculation of *Fo* and *Mi* at 14 DAI. The greatest reduction in total chlorophyll content of 52.3% was noted in leaves of G. maofen 802 variety after combined application of *Fo* and *Mi*. Solo applications of *Fo* and *Mi* showed reductions of 36% and 2.4%, respectively. Zhongza 09 showed little change in total chlorophyll content after exposure to all treatments as compared to control (Figure 1D).

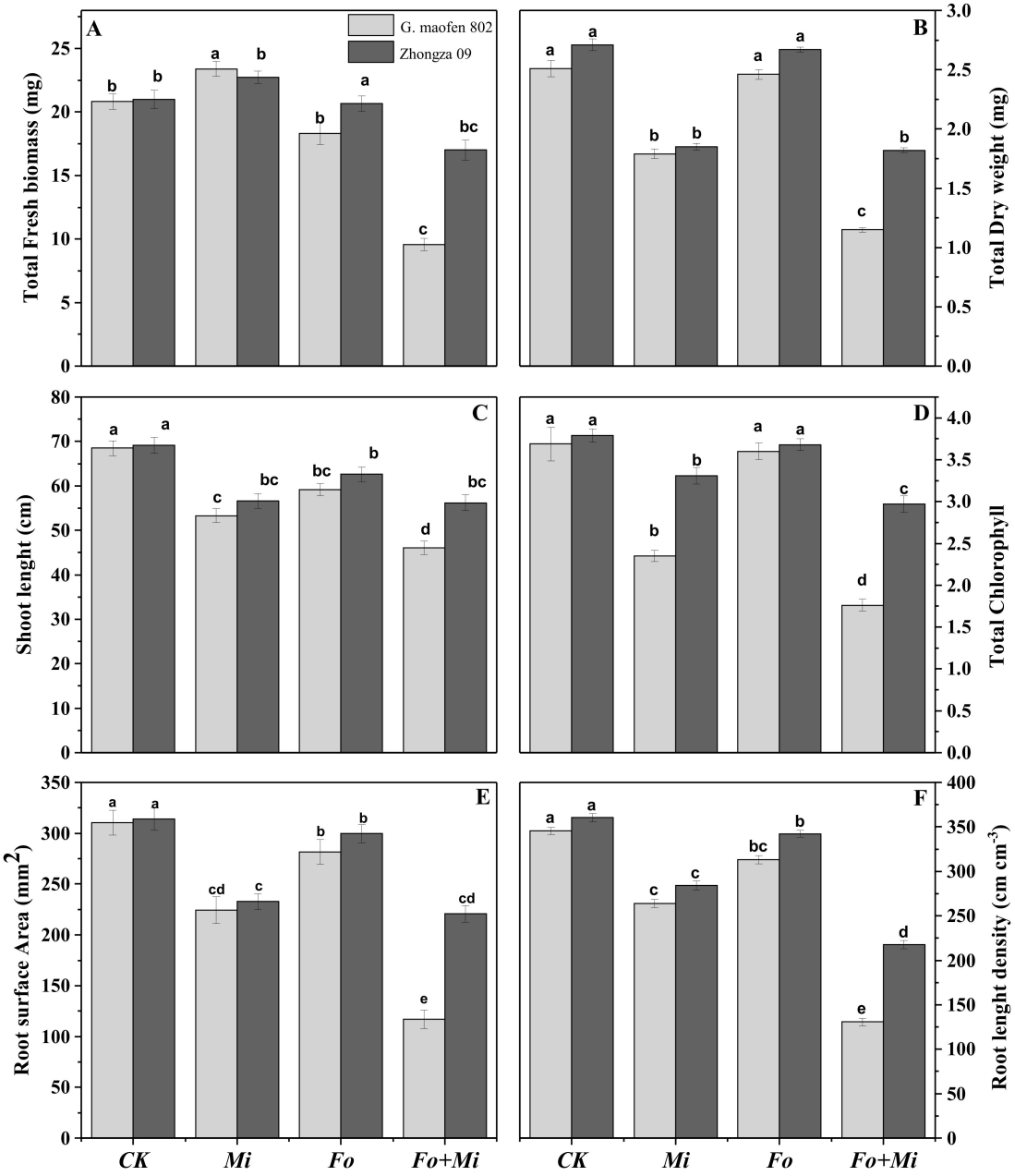

Figure 1. Effects of *Fusarium oxysporum* and *Meloidogyne incognita* alone and in combination on the growth (**A**–**C**) and physiological (**D**) and root (**E**,**F**) attributes of two tomato cultivars (G. maofen 802 and Zhongza 09) at 14 days after inoculation (DAI) under greenhouse conditions. Note: CK, non-inoculated control; *Fo*, *Fusarium oxysporum*; *Mi*, *Meloidogyne incognita*; *Fo* + *Mi*, *Fusarium oxysporum* + *Meloidogyne incognita*. Bars showing dissimilar lower-case letters are statistically different from each other at $p \leq 0.05$ (Tukey–Kramer test). Values are mean ± SE.

3.4. Interactive Effect of Fo and Mi on Photosynthetic Traits

The results further showed that combined *Fo* and *Mi* application produced maximum reductions in photosynthetic capacity (Pn), transpiration rate (Tr), and stomatal activity (gs) of 70%, 78%, and 86%, respectively, in G. maofen 802 variety as compared to control. Contrarily, internal carbon dioxide concentration (Ci) was increased by 39% as compared to control in G. maofen 802 after combined inoculation with *Fo* and *Mi*. In the case of solo *Mi* treatment, Tr and Ci were increased in both varieties by 20% and 23%, respectively, as compared to control. The *Fo* application influenced the Ci levels of G. maofen 802 and Zhongza 09 (3.5% and 1.4%, respectively) as compared to control (Figure 2).

Chlorophyll fluorescence, electron transport rate, photosystem II (PSII), and Fv/Fm were significantly influenced by *Fo* and *Mi* application in both varieties, except for in the control.

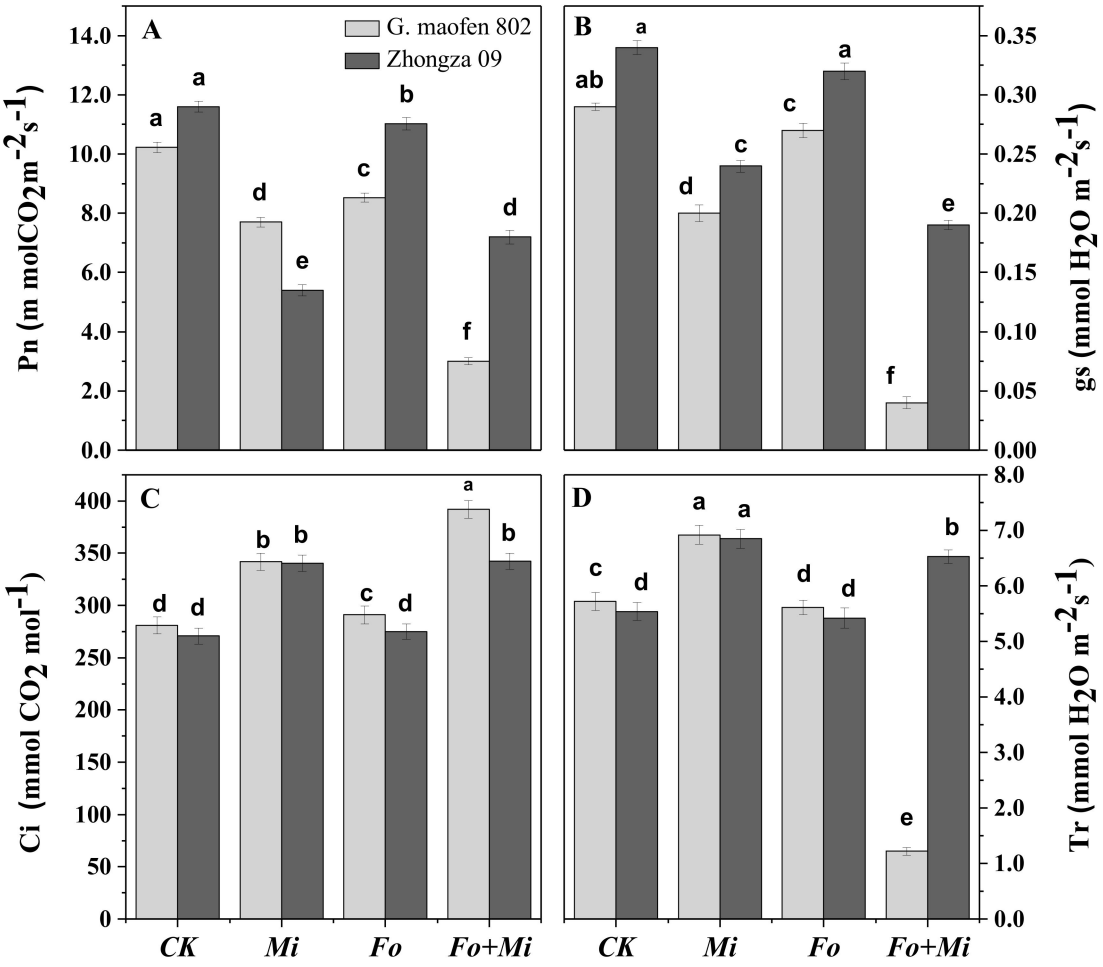

Figure 2. Effects of *Fusarium oxysporum* and *Meloidogyne incognita* alone and in combination on photosynthetic parameters of two tomato cultivars (G. maofen 802 and Zhongza 09) at 14 DAI in greenhouse conditions: (**A**) net photosynthesis (Pn), (**B**) stomatal conductance (gs), (**C**) intracellular carbon dioxide (Ci), and (**D**) transpiration rate (Tr). Bars showing dissimilar lower-case letters are statistically different from each other at $p \leq 0.05$ (Tukey–Kramer test). Values are mean ± SE.

Both G. maofen 802 and Zhongza 09 varieties had higher chlorophyll fluorescence traits with *Mi* application. In G. maofen 802 variety, the *Mi* treatment caused increases of 7.9%, 9.8%, 24.4%, and 13.0% in YII, Fv/Fm, qP, and ETR, respectively, compared to non-inoculated plants. The minimum values for chlorophyll fluorescence traits, YII (55.5%), Fv/Fm (36.6%), qP (64.7%), and ETR (17.7%) were noted in G. maofen 802 with the combined inoculation of both pathogens as compared with control. Similarly, under *Fo* inoculation, considerable reductions of 15.0%, 8.4%, 11.7%, and 8.8% were observed in YII, Fv/Fm, qP, and ETR, respectively, compared with control. Zhongza 09 showed minimum reductions of photosynthetic parameters of 20%, 16%, 29%, and 10% for YII, Fv/Fm, qP, and ETR, respectively, with dual inoculation of *Fo* and *Mi* as compared with control (Figure 3).

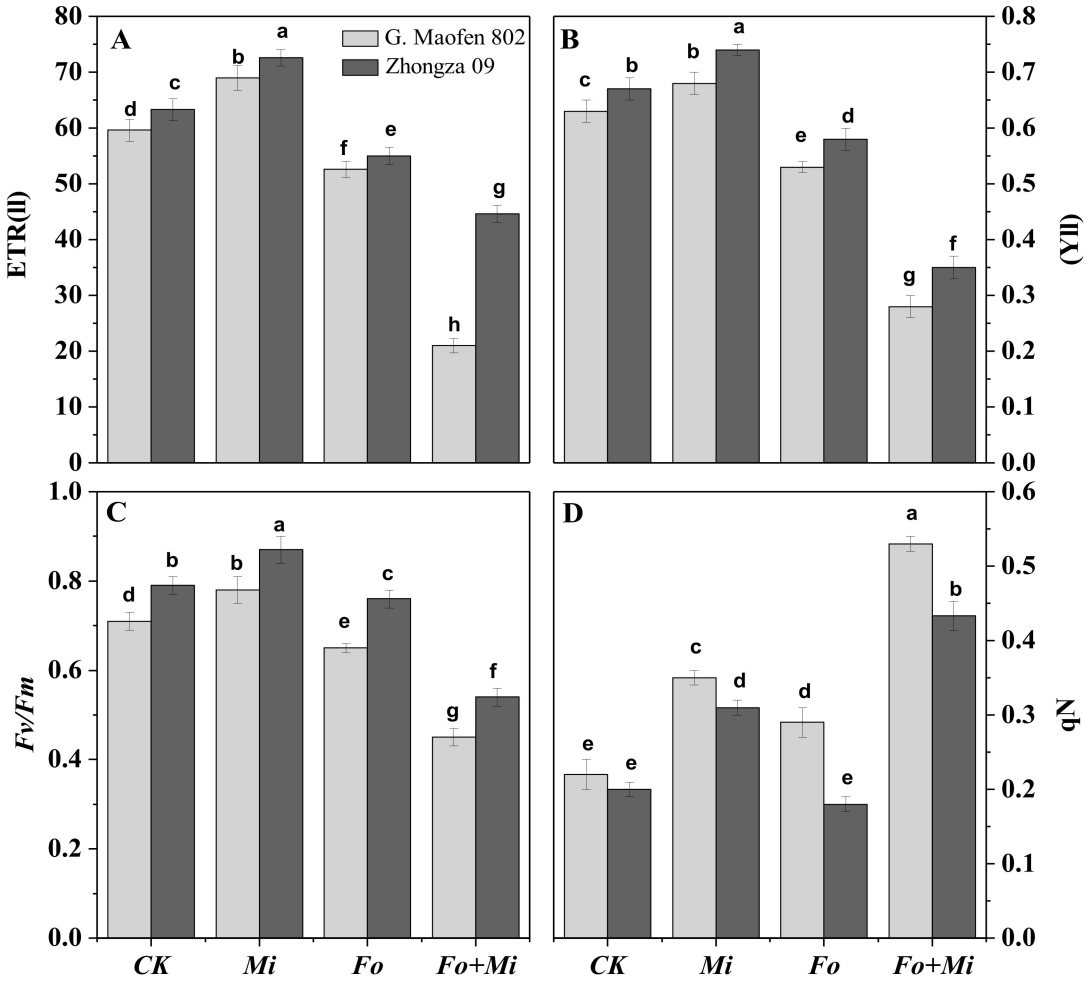

Figure 3. Effects of *Fusarium oxysporum* and *Meloidogyne incognita* alone and in combination on chlorophyll fluorescent parameters of two tomato cultivars (G. maofen 802 and Zhongza 09) under greenhouse conditions at 14 DAI: (**A**) the electron transport rate of PSII (ETR), (**B**) PSII quantum yield of light (YII), (**C**) potential quantum yield of photosystem II (Fv/Fm), and (**D**) non-photochemical quenching coefficient (qN). Bars showing dissimilar lower-case letters are statistically different from each other at $p \leq 0.05$ (Tukey–Kramer test). Values are mean ± SE.

3.5. Interactive Effect of Fo and Mi on Oxidative Defense Mechanism in Leaves and Roots

Antioxidants were significantly influenced in both varieties with single and concomitant treatment of *Fo* and *Mi*. Compared with control, combined application of *Fo* and *Mi* induced higher MDA (265% and 342%, respectively) and H_2O_2 (189% and 194%, respectively) contents in tomato roots and leaves of G. maofen 802 than Zhongza 09 (Figure 4). However, *Mi* treatment in tomato roots and leaves induced less MDA and H_2O_2 contents in both cultivars than combined inoculation with *Fo*. Furthermore, under the concomitant infestation of *FO* and *Mi*, relatively higher concentrations of polyphenol oxidase (PPO) (91%), ascorbate oxidase (AAO) (15%), ascorbate peroxidase (APX) (12%), sodium dismutase (SOD) (52.7%), catalase (CAT) (41%), and proteins (79.4%) were found in leaves of Zhongza 09 compared with G. maofen 802. Interestingly, compared to control in G. maofen 802, *Mi* treatment alone increased the contents of SOD (18% and 37%, respectively), PPO (17% and 35%, respectively), and APX (9.9% and 24%, respectively) in roots and leaves (Table 2). Contrarily, AAO and protein contents were reduced in both varieties in roots and leaves when treated with *Mi* alone and in combination with *Fo*.

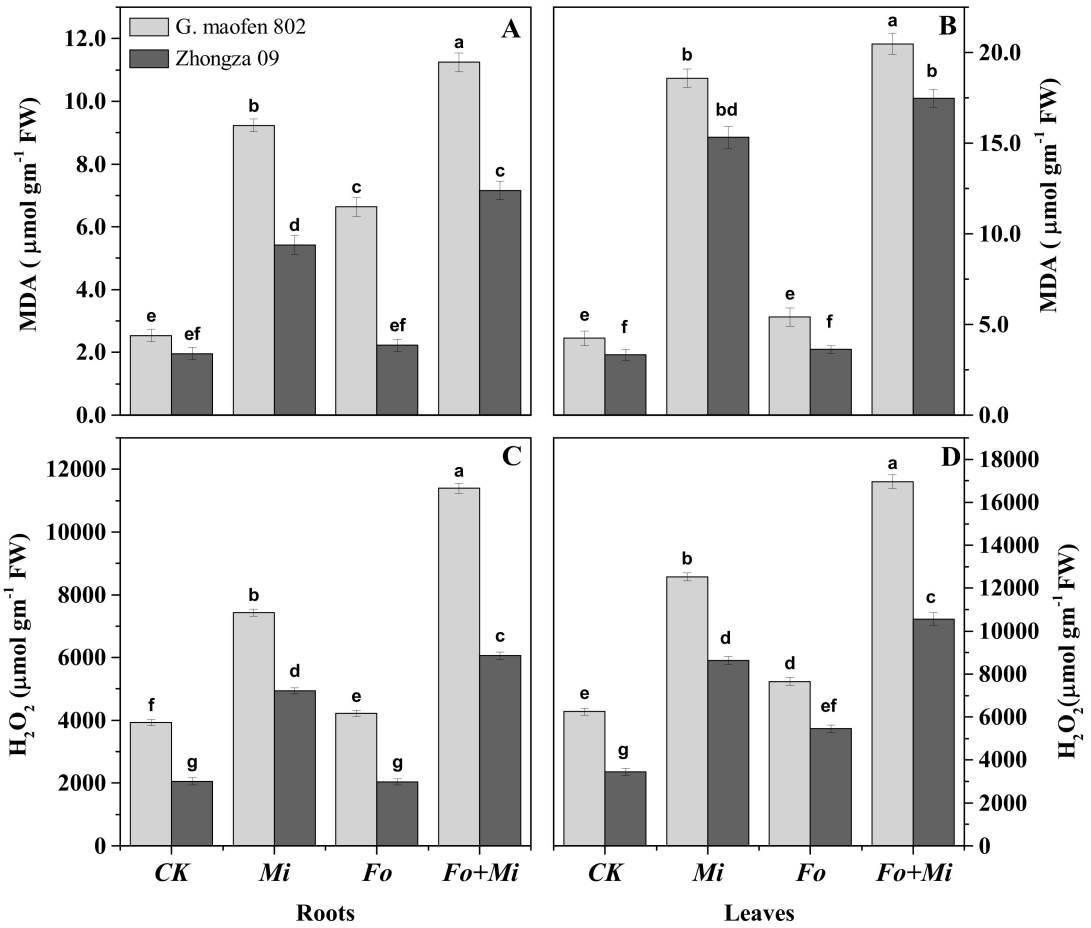

Figure 4. Effects of *Fusarium oxysporum* and *Meloidogyne incognita* alone and in combination on oxidative stress responses of two tomato cultivars (G. maofen 802 and Zhongza 09) under greenhouse conditions at 14 DAI.: (**A**) malondialdehyde (MDA) contents in roots, (**B**) malondialdehyde (MDA) contents in leaves, (**C**) hydrogen peroxide (H_2O_2) contents in roots, and (**D**) hydrogen peroxide (H_2O_2) contents in leaves. Bars showing dissimilar lower-case letters are statistically different from each other at $p \leq 0.05$ (Tukey–Kramer test). Values are mean ± SE.

Table 2. Effects of *Fusarium oxysporum* and *Meloidogyne incognita* alone and in combination on antioxidants of two tomato cultivars (G. maofen 802 and Zhongza 09) under greenhouse conditions after 14 days.

Plant Parts	Cultivars	Treatments	Superoxide Dismutase (Unit mg^{-1} Protein)	Catalase (Unit mg^{-1} Protein)	Polyphenol Oxidase (Unit mg^{-1} Protein)	Ascorbate Peroxidase (Unit mg^{-1} F.W)	Ascorbate Oxidase (Unit mg^{-1} Protein)	Proteins (mg g^{-1} F.W)
Leaves	G. maofen 802	*CK*	8.06 ± 0.15 e	8.93 ± 0.15 c	2.15 ± 0.04 f	9.56 ± 0.17 f	0.591 ± 0.04 d	1.61 ± 0.03 c
		Mi	9.54 ± 0.17 b	6.63 ± 0.12 g	2.53 ± 0.03 d	13.3 ± 0.16 c	0.442 ± 0.05 f	1.53 ± 0.04 d
		Fo	7.18 ± 0.16 f	7.45 ± 0.13 e	1.86 ± 0.03 g	12.4 ± 0.14 d	0.622 ± 0.03 b	1.5 ± 0.03 e
		Fo + Mi	2.33 ± 0.12 h	2.75 ± 0.04 h	0.15 ± 0.01 h	5.083 ± 0.13 g	0.323 ± 0.01 h	0.28 ± 0.01 h
	Zhongza 09	*CK*	8.24 ± 0.16 d	9.43 ± 0.14 b	2.25 ± 0.05 c	10.32 ± 0.18 e	0.604 ± 0.03 c	1.98 ± 0.04 b
		Mi	11.34 ± 0.13 a	8.23 ± 0.13 d	3.43 ± 0.03 a	12.56 ± 0.16 d	0.535 ± 0.04 e	1.4 ± 0.03 f
		Fo	8.83 ± 0.17 c	10.64 ± 0.11 a	2.83 ± 0.04 b	14.72 ± 0.13 a	0.784 ± 0.03 a	2.03 ± 0.03 a
		Fo + Mi	6.73 ± 0.13 g	6.75 ± 0.17 f	2.22 ± 0.03 e	13.85 ± 0.15 b	0.422 ± 0.04 g	1.01 ± 0.02 g
Roots	G. maofen 802	*CK*	4.19 ± 0.16 g	6.83 ± 0.12 d	1.25 ± 0.02 e	5.66 ± 0.15 d	0.351 ± 0.03 d	1.21 ± 0.03 d
		Mi	5.76 ± 0.15 e	5.67 ± 0.11 f	0.94 ± 0.03 f	4.28 ± 0.14 g	0.232 ± 0.02 f	0.85 ± 0.04 f
		Fo	6.61 ± 0.16 c	6.35 ± 0.14 e	1.6 ± 0.02 c	6.23 ± 0.14 b	0.427 ± 0.04 b	0.93 ± 0.05 e
		Fo + Mi	1.20 ± 0.10 h	1.87 ± 0.01 g	0.3 ± 0.04 g	1.99 ± 0.16 h	0.125 ± 0.05 h	0.03 ± 0.01 g
	Zhongza 09	*CK*	4.85 ± 0.14 f	7.54 ± 0.12 b	1.77 ± 0.05 b	5.94 ± 0.14 c	0.406 ± 0.03 c	1.43 ± 0.02 b
		Mi	7.54 ± 0.15 b	7.1 ± 0.13 c	1.43 ± 0.03 d	5.53 ± 0.12 e	0.335 ± 0.02 a	1.13 ± 0.04 c
		F0	8.48 ± 0.13 a	8.25 ± 0.13 a	1.84 ± 0.04 a	6.75 ± 0.15 a	0.55 ± 0.04 e	1.82 ± 0.03 a
		Fo + Mi	5.94 ± 0.11 d	5.66 ± 0.1 f	0.83 ± 0.02 f	4.73 ± 0.12 f	0.246 ± 0.02 g	0.95 ± 0.01 e

All the data presented are the mean ± SE of three replications. The different lower-case letters within a column indicate significant differences ($p < 0.05$) among *Mi*, *Fo*, and *Fo + Mi* treatments compared with control, as assessed by Tukey–Kramer test.

3.6. Proline Contents and Electrolyte Leakage

The combined application of *Fo* and *Mi* on both varieties significantly increased the electrolyte leakage and proline contents in roots and leaves (Figure 5). Proline content values were higher in roots than shoots, while maximum electrolyte leakage was observed in leaves after combined infestation of *Fo* + *Mi* in G. maofen 802 followed by *Mi* infestation as compared with control. In *Fo* application, a small increase of proline and electrolyte leakage was recorded.

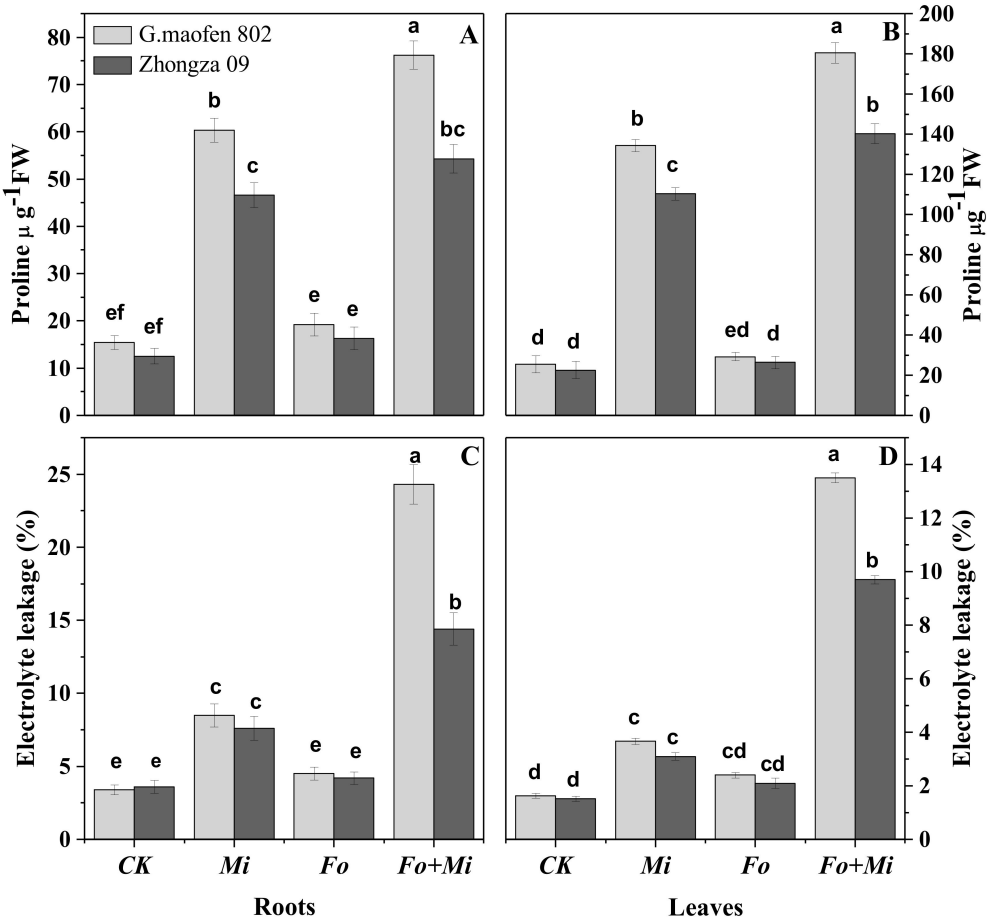

Figure 5. Effects of *Fusarium oxysporum* and *Meloidogyne incognita* alone and in combination on proline contents (**A**,**B**) and electrolyte leakage (**C**,**D**) of two tomato cultivars (G. maofen 802 and Zhongza 09) under greenhouse conditions at 14 DAI. Bars showing dissimilar lower-case letters are statistically different from each other at $p \leq 0.05$ (Tukey–Kramer test). Values are mean ± SE.

3.7. Root Galls and Mi Population in Roots and Soil

Mi population (eggs and females) and galling index values demonstrated clear variations in tomato roots. Galling index, number of eggs, females in 1 g root samples, and juveniles per 250 cm^3 soil (3, 870, 66, 538 for G. maofen 802) and (2, 675, 45, 492 for Zhongza 09) respectively were assessed by dual infestation of *Mi* and *Fo* after 35 days (Table 3). The co-inoculation of both pathogens either concurrently or sequentially showed little or similar response for both varieties. The highest number of eggs, highest galling index value, and highest number of females in roots were recorded with *Mi* single application in both varieties. In the sequential applications, *Fo* infestation before *Mi* showed a lower galling index value than the second-stage juveniles, while *Mi* application before *Fo* showed an equivalent response to the concomitant application of *Fo* and *Mi* in G. maofen 802 and Zhongza 09 (Table 3). These results revealed that several females were adversely affected by combined inoculation with *Fo*, either sequentially or at the same time.

Table 3. Effects of *Fusarium oxysporum* and *Meloidogyne incognita* alone and in combination on two tomato roots of G. maofen 802 and Zhongza 09 cultivars under greenhouse conditions after 35 days.

Varieties	Treatments	No. of Females (Per g Root)	Root Population		Soil Population	
			No. of Eggs (Per g Root)	Galling Index (0–5)	Size of Galls (mm)	No. of Juveniles (Per 250 cm^3 Soil)
G. maofen 802	CK	0.0	0.0	0.0	0.0	0.0
	Mi	83 ± 3.5 a	11445 ± 10 a	5.0	3.8 ± 0.1 a	644 ± 5 a
	Fo	0.0	0.0	0.0	0.00	0.0
	Fo + *Mi*	66 ± 2.5 b	870 ± 8 c	3.0	1.8 ± 0.2 c	538 ± 13 b
	$Fo \xrightarrow{\text{After7days}} Mi$	51 ± 1.5 cd	755 ± 12 d	2.0	1.6 ± 0.1 c	480 ± 8 cd
	$Mi \xrightarrow{\text{After7days}} Fo$	64 ± 2.6 b	875 ± 6.5 c	3.0	1.7 ± 0.2 c	541 ± 5 b
Zhongza 09	CK	0.0	0.00	0.0	0.0	0.0
	Mi	56 ± 2.0 c	957 ± 17 b	3.0	2.2 ± 0.1 b	558 ± 6 b
	Fo	0.0	0.0	0.0	0.00	0.0
	Fo + *Mi*	45 ± 2.6 d	675 ± 6 e	2.0	1.1 ± 0.1 d	492 ± 6 c
	$Fo \xrightarrow{\text{After7days}} Mi$	36 ± 1.5 e	564 ± 18 f	1.0	1.0 ± 0.1 d	409 ± 5 e
	$Mi \xrightarrow{\text{After7days}} Fo$	46 ± 2.5 d	683 ± 6 e	2.0	1.2 ± 0.18 d	490 ± 7 c

All the data presented are the mean ± SE of three replications. The different lower-case letters within a column indicate significant differences at $p \leq 0.05$ (Tukey–Kramer test) among the concurrent and sequential *Mi* and *Fo* treatments in greenhouse conditions compared with control at 35 DAI.

3.8. Transmission Electron Microscopy Results

The presence of typical hyphae and ultrastructure changes were observed in the roots of tomato plants with single and combined application of *Fo* and *Mi* as compared to control (Figure 6). We found unique tetrahedral crystalline bodies (TCB) in root cells of Zhongza 09 cultivar after *Fo* and *Mi* single and combined applications (Figure 6C,E,F). The mycelium of *Fo* were clearly observed under TEM in entire root cells, along with new entry points in cell walls of G. maofen 802 after *Fo* + *Mi* application (Figure 6E). In the control (Figure 6A,B) for both cultivars, no TCB bodies were found. The unique TCB structure was enveloped within a membrane near mitochondria (Figure 6H).

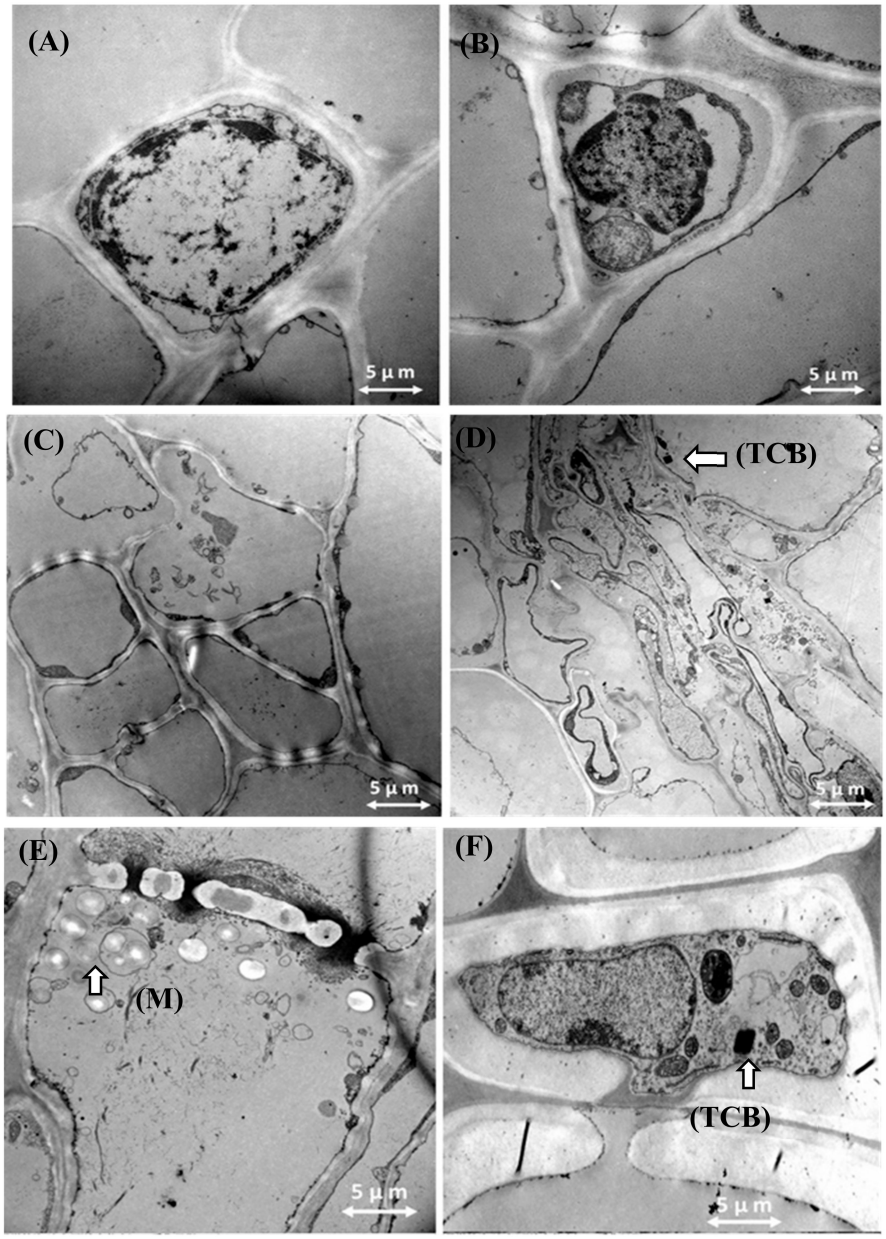

Figure 6. *Cont.*

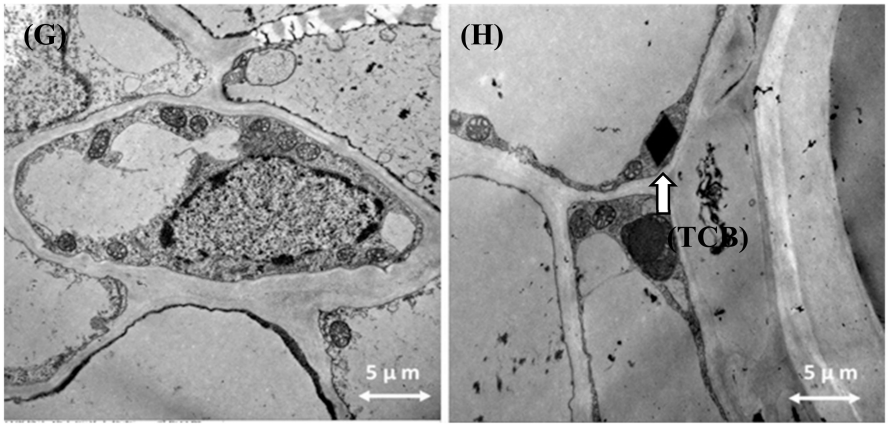

Figure 6. Effects of *Fusarium oxysporum* and *Meloidogyne incognita* alone and in combination on the anatomical structure of the roots of two tomato cultivars (G. maofen 802 and Zhongza 09) under TEM: (**A**) the healthy root cells of G. maofen 802; (**B**) healthy root cells of Zhongza 09 as control; (**C**) root cells of G. maofen 802 after *Mi* application; (**D**) root cells after *Mi* application in Zhongza 09 with TCB structure; (**E**) roots of G. maofen 802 after *Fo* + *Mi* application with mycelium (M) inside the cell; (**F**) root cells of Zhongza 09 after *Fo* and *Mi* application with TCB structure; (**G**) root cells of G. maofen 802 after single application with no TCB; (**H**) root cells of Zhongza 09 after single application of *Fo* showing unique crystalline structure near mitochondria. Note: TCB, tetra hedral crystalline bodies; M, mycelium.

4. Discussion

Plant protection measures in the past have focused predominantly on single-host–single-disease interactions. However, in nature, plant infection often involves multiple species or genotypes. The multiple pathogens combine as a disease complex on various crops. Moreover, tracheomycosis diseases block the intranet system of the plant, which transports nutrients and water. The present investigation highlights the issue of hyperparasitism, resulting in destruction of tomato seedlings after infestation of two soil-borne disease-causing agents, *Fusarium oxysporum* (*Fo*) and *Meloidogyne incognita* (*Mi*). The *Fusarium oxysporum* distorts the root system by blocking vascular bundles with tylosis and root-knot nematodes, parasitizing roots of important crops and causing huge economic losses in agriculture globally. In order to control plant diseases, different approaches such as resistant cultivars, biological agents, cultural practices, and agrochemical control have been used in the field [43]. Previously, researchers found pathogen synergy in susceptible cultivars. However, here we selected two such commercial hybrid cultivars that are resistant against *Fo* but susceptible to *Mi* to perceive the synergism and viability of *Fo*-resistant cultivars.

Disease involves a complex interplay between a host plant and a pathogen, and the resistance–susceptibility response can involve several components, such as the plant's defense mechanism, the environment, and the virulence of pathogens [44]. Plant-parasitic nematodes in the genus *Meloidogyne incognita* are strongly associated with wilt symptoms assumed to be caused by the fungus *F. oxysporum*. According to our results, G. maofen 802 cultivar lost its potential and showed chlorotic disease symptoms within 14 days of co-inoculation with *Mi*. Zhongza 09 maintained tolerance against *Fo* expression but its physiological traits were significantly affected. *Mi* application alone and in combination with *Fo* impeded all plant growth parameters in both cultivars (Figure 1A–C). Our results are strengthened by previous findings. Fusarium wilt on tomato plants transformed into the most devasting disease in combined infection with root-knot nematode [45]. *Rhizoctonia* root rot was the more severe in the presence of *Meloidogyne incognita* in green beans [46]. Sever symptoms on aerial parts of olive plants were observed when a non-defoliant strain of the fungus (SS-4) of *Verticillumdhaliae* and the root-knot nematode were inoculated simultaneously [47]. The 100% severity of chlorotic symptoms at 14 DAI on the foliage was observed after combined application of *Mi* and *Fo*

followed by sequential application of *Mi* 7 days prior to *Fo* (95.1%) in G. maofen 802. Mallaiha et al. [48] reported that inoculation of root lesion nematodes prior to *Fusarium* spp. caused maximum disease incidence in *Crossandra* species. Fusarium wilt incidence drastically increased when *M. incognita* was inoculated with *F. oxysporum* and *F. spnivem*, and also decreased the potential of Fusarium wilt varieties of watermelon [49]. This may be due to the entrance of *Fo* with endoparasites (*Mi)* at the same time and prior to *Mi.* Mai et al. [50] reported that root galls and giant cells induced by *Mi* often made suitable sites for pathogenic and non-pathogenic soil-borne fungal species. The number and size of root galls increased in single inoculation of *Mi* compared with in combination with *Fo* (Supplementary Figure S2). In single inoculation, the penetration of second-stage juveniles (J2) in roots was more attainable as they had no competition. Significant reductions in galling index and nematode populations in the soil and roots were observed in concurrent application of *Fo* and *Mi*, followed by sequential application of *Mi* prior to *Fo* (Table 2). These results are strengthened by the findings of Hua et al. [49], showing that co-inoculation of *M. incognita* and *F. oxysporum* led to an early development of Fusarium wilt, and that nematode populations were reduced in the presence of fungus. Moreover, *Fo* might cause cottony growth over the lateral roots [51], leading to these roots becoming inappropriate for juvenile invasion. These results are further substantiated by the findings of Pshibytko et al. [52].

Moreover, *Fo* produced several mycotoxins and fusaric acid in the xylem and phloem vessels after successful development in roots of tomato, causing certain morphophysiological disorders, as previously noted by Singh et al. [11]. Under such conditions, the *Mi* population migrates into the soil after the enhancement of their reproduction in this hostile condition. On the other hand, *Mi* introduced several compounds into the roots, such as flavonoids and proteins; and also introduced carbohydrates into the root galls, exciting the other soil-borne pathotypes that cause disease. Similar findings were reported by Al-Hazm et al. [46] in green beans roots.

The enhancement of wilt severity due to nematode co-infection is probably related to physiological and anatomical changes induced by nematode infection in root cells. The plant root cells have a dynamic structure and composition (phenolics and proteins) that can be remodeled in response to biotic and abiotic stress [53]. The transmission electron microscopy results of tomato root cells of both cultivars (G. maofen 802 and Zhongza 09) showed a clear difference in response to co-inoculation of *Fo* and *Mi* (Figure 6E,F). Our results showed that novel tetrahedral crystalline bodies (TCB) appeared in root cells of Zhongza 09 after inoculation of *Fo* alone, *Mi* alone, and combined inoculation, while these tetra-structures were absent in G. maofen 802 in all treatments (Figure 6C,E,G). These tetrahedral crystalline structures (which had not been reported before) might be due to the large set of modifying proteins present in the root cells, which were activated in response to pathogens and altered cell wall composition to show defensive responses [54]. Bleve-Zacheo et al. [55] witnessed a number of globular crystalline bodies (proteins) together with starch accumulation in *Mi*-mediated gene varieties. The root area density and length are directly related to the photosynthetic machinery (light-capturing organ, PSII center, and efficiency of photochemical energy use) [56]. Therefore, leaf photosystems and root systems work together to promote the growth and yield of crops by efficiently using water and nutrients. Water deficit and nutrient shortages ultimately damage the photosynthetic pigments and activity of PSII [57]. As a result, chlorotic lesions were observed on leaves.

In both varieties, significant changes in root morphology directly influenced the physiological parameters after co-inoculation with *Fo* and *Mi* and with a single application of *Mi*. Furthermore, the successful synergism of *Fo* + *Mi* had a negative correlation with biomass accumulation, although root weight and diameter increased due to gall formation. More specifically, a profound reduction in total fresh and dry biomass, photosynthetic rate, stomatal conductance, transpiration rate, chlorophyll fluorescence, and non-photosynthetic quenching was detected in our experiment at 14 DAI by co-inoculation of *Fo* and *Mi* in both cultivars in comparison to control and single inoculation (Figure 2, Figure 3). Photosynthetic traits are directly proportional to plant growth and development [58]. Among them, chlorophyll contents are key components of photosynthesis, through which plants derive their energy for metabolism and growth [59]. Chlorophyll contents are sensitive to biotic and

abiotic stress [60] and ultimately directly affect the plant health [61]. Previous studies have shown that infection of plants by *M. incognita* and F. oxysporum can result in reduced chlorophyll content and photosynthesis [62,63]. In the current results, total chlorophyll contents were decreased in each treatment as compared to control (Figure 1D). There is a correlation between photosynthetic efficiency and chlorophyll pigments. The photosynthetic efficiency of photosystem II (measured by the F_v/F_m value) is a reliable indicator of plant adaptation to stress [64]. In the present study, chlorophyll fluorescence parameters, F_v/F_m, ETR, and YII values were seriously reduced by co-inoculation of *Fo* and *Mi* (Figure 3). Intriguingly, all photosynthetic traits were significantly increased after *Mi* inoculation in both cultivars, while the qN value increased as disease progressed. These results are consistent with findings by Zhou et al. [65], who also reported significant reduction in F_v/F_m levels of tomato plants due to biotic stress. Contrarily, all photosynthetic traits except gaseous exchange were higher in *Mi* treatment at 14 DAI. Earlier, Ping et al. [63] determined that *M. incognita* did not consistently cause damage to photosystem II in all cultivars of cotton. These effects increase with the duration of time [66]. The plants' lack of above-ground symptoms, along with the low degree of root galling, may be attributed to the lower population of J2. However, over time the nematode population density increased and above-ground symptoms appeared on the plants [67]. Furthermore, recent studies by Ramalingam et al. [45] and Meena et al. [68] confirmed that the co-infection with *Mi* and *Fo* significantly disturbed the photosynthetic traits of tomato and *Dianthus caryophyllus*, respectively, under greenhouse conditions. In our results, the photosynthetic rate decreased even though the internal carbon dioxide (Ci) concentration and transpiration rate increased with co-inoculation of *Fo* and *Mi* (Figure 2A–C), indicating that the decrease in photosynthetic rate (Pn) was not caused by reduction in transpiration rate (Tr) and internal carbon dioxide (Ci) concentration. Therefore, this reduction in photosynthetic rate must have been caused by non-stomatal factors, such as photosynthetic light reactions and Calvin cycle biochemistry [69]. These reductions might be attributed to disturbed physiological functions of plants [70]. ROS generation is one of the major biotic and abiotic stress indicators in plants. Photosystem II activity is directly related to ROS generation by the involvement of calcium-signaling-mediated kinase cascades [71,72]. Overgeneration of ROS can produce massive amounts of MDA in cell membranes, resulting in an oxidative burst at the subcellular level [73]. In our study, both varieties substantially accumulated malondialdehyde (MDA), hydrogen peroxide (H_2O_2), and proline contents, in addition to increased electrolyte leakage in roots and leaves after synergistic treatment of *Fo* + *Mi* compared with single inoculation of *Mi* (Figure 5C,D). These findings are in line with Kesba et al. [74]. H_2O_2 is the most common ROS produced in plants in response to the invasion of nematodes, fungi, and bacteria, and affects various growth phenotypes of plants [75,76]. In resistant varieties, several defense-related antioxidants (superoxide dismutase (SOD), catalase (CAT), polyphenol oxidase (PPO), ascorbate peroxidase (APX), and ascorbate oxidase (AAO)) were produced to reduce the concentration of the hydrogen peroxide (H_2O_2) and malondialdehyde (MDA). Moreover, it might be due to the presence of antioxidants (SOD, PPO, CAT, APX, and AAO) that Zhongza 09 did not show *Fo* expression in conjunction with *Mi*. Therefore, there is a negative correlation between H_2O_2 and defense-related enzymes in that variety (Table 3). CAT is primarily responsible for hydrolyzing H_2O_2 into water (H_2O) and oxygen (O_2) [64]. According to our results, CAT activity was maximal in *Fo*-resistant plants, while *Mi* application induced slightly more CAT activity than control in both leaves and roots. In contrast, co-inoculation of *Fo* + *Mi* in both varieties reduced the catalase activity. Previously, Molinari et al. [77] reported no effects on CAT activity in nematode-susceptible cultivars. Contrarily, Eissa et al. [78] suggested that nematode-resistant cultivars without inoculation had a higher concentration of CAT than susceptible cultivars. This contradiction might be due to the fact that the nematode population did not reach a certain level where CAT activity could be highly reduced. SOD prevents injurious effects of O_2^- radicals in plant cells and converts these into hydrogen peroxide, which is then transferred into H_2O and O_2 by catalase activity [79]. PPO activity is responsible for metabolism and modifies phenols into quinone in plants to scavenge biotic stressors [80]. Higher production of PPO may induce the production of PR proteins, which are directly involved in resistance

mechanisms in plants by overcoming the infection of pathogens in plant tissues [81]. Our results revealed that accumulated SOD enzymes and phenolic compounds were more alleviated in leaves of *Mi*-treated plants than *Fo*-inoculated plants. Contrarily, in roots, SOD accumulation was more obvious in *Fo*-resistant plants in both cultivars than *Mi*-treated and untreated plants. Combined inoculation with *Fo* + *Mi* in G. maofen 802 induced less activity of SOD and PPO in roots and leaves than Zhongza 09 (Table 3). Our findings are supported by the results of Sharma et al. [6], who reported that PPO activity was increased in tomato PT3 after dual inoculation of plant growth promoter rhizobacteria (PGPR) and mycorrhiza against *Mi.* Awan et al. [82] reported that groups of tomatoes resistant against *Alternaria solani* had higher concentrations of PPO, CAT, and POD than susceptible groups. According to Arshad et al. [83], ascorbic acid contents of plants are directly related to resistance against pathogens. APX and AAO are chloroplastic or cytosolic enzymes that metabolize the activity of H_2O_2 in different cell compartments and are intricately involved in the homeostasis of AsA and balancing of ROS generation [84]. The maximum value of APX was measured in leaves infested with *Mi* in G. maofen 802 and Zhongza 09, while the minimum concentration of APX was observed in roots and leaves of both cultivars after co-inoculation of *Fo* + *Mi*. These findings are strengthened by the results from Yang et al. [85], where a higher concentration of ascorbate peroxidase was found in resistant cultivars of tomato. Proteins play a major role in cell function and structure. Protein contents were significantly depleted in all treatments. Only untreated plants showed higher concentrations of proteins in roots and leaves in both varieties at 14 days. Maximum depletion was found in concurrent treatment with *Fo* + *Mi* and minimum depletion was found with *Fo* application. Previously, McGovern et al. [86] observed a low quantity of proteins in tomato roots and leaves infected with Fusarium wilt.

5. Conclusions

In order to make significant progress in plant disease management, research efforts should made to develop suitable strategies to manage multiple pathogen infestations. The role of pathogen–pathogen interactions and their impact on plant defense systems should increasingly be recognized as having equal importance as studying single plant–pathogen interactions. Our circumstantial evidence suggests that *Fo* + *Mi* combined infestation in roots significantly reduced the growth, photosynthetic traits, physiological attributes, and defense-related enzymes by exaggerating oxidative damage as compared to control in tomato plants, ultimately leading to death in a few days, while single *Mi* inoculation in plants did not significantly reduce the morphological and physiological attributes at 14 DAI. In the current study, we found that the *Fo*-resistant cultivar lost its vitality after co-inoculation with *Mi*. Tolerant cultivars adopt different mechanistic strategies at structural and cellular levels to sustain the biotic stress. Furthermore, the study provides valuable results regarding the synergistic interaction of *Fo* and *Mi*, encouraging the design of effective ameliorative strategies that can be used in future breeding programs to produce commercial resistant varieties, as well as for the formulation of pesticides for the effective management of these two pathogens together. However, future research is needed to elucidate the molecular vision of interaction between *Fusarium oxysporum* and *M. incognita*.

Supplementary Materials: The following are available online at http://www.mdpi.com/2073-4395/10/2/159/s1: Figure S1: Effect of *Fusarium oxysporum* and *Meloidogyne incognita* on foliar part of G. maofen 802 at 14 DAI, Figure S2: Effect of *Fusarium oxysporum* and *Meloidogyne incognita* single and combine application on roots of G. maofen 802 after 35 DAI, Table S1: Tomato cultivars used for screening against *Fo* and *Mi,* Table S2: Screening of tomato cultivars against *Fusarium oxysporum* and *Meloidogyne incognita.*

Author Contributions: Conceptualization, A.M., J.-T.C., and H.W.; methodology, A.M. and N.T.T.H.; software, A.M., N.T.T.H., M.K., Q.H., and A.M.; validation, H.W., A.M., J.-T.C., and H.A.; formal analysis, A.M.; investigation, Q.H. and K.T.; resources, H.W.; data curation, A.M. and K.T.; writing—original draft preparation, A.M. and M.K.; writing—review and editing, A.M., M.K., S.A., A.M., and H.A.; supervision, H.W. All authors have read and agreed to the published version of the manuscript.

Acknowledgments: We express our sincere gratitude to Guangxi Innovation Team of National Modern Agricultural Technology System (nycytxgxcxtd-10-04), the National Natural Science Foundation of China (31660511), Construction project of characteristic specialty and experimental training teaching base (Center)—characteristic specialty—Plant Protection (2018–2020).

Conflicts of Interest: The authors declare that the research was conducted in the absence of any commercial or financial relationship that could be construed as a potential conflict of interest.

References

1. Li, X.; Lewis, E.E.; Liu, Q.; Li, H.; Bai, C.; Wang, Y. Effects of long-term continuous cropping on soil nematode community and soil condition associated with replant problem in strawberry habitat. *Sci. Rep.* **2016**, *6*, 30466. [CrossRef] [PubMed]
2. Chen, M.; Li, X.; Yang, Q.; Chi, X.; Pan, L.; Chen, N.; Yang, Z.; Wang, T.; Wang, M.; Yu, S. Soil eukaryotic microorganism succession as affected by continuous cropping of peanut-pathogenic and beneficial fungi were selected. *PLoS ONE* **2012**, *7*, e40659. [CrossRef] [PubMed]
3. Ali, M.A.; Naveed, M.; Mustafa, A.; Abbas, A. The good, the bad, and the ugly of rhizosphere microbiome. In *Probiotics and Plant Health*; Springer: Berlin, Germany, 2017; pp. 253–290.
4. Gordon, T.R. *Fusarium oxysporum* and the Fusarium wilt syndrome. *Annu. Rev. Phytopathol.* **2017**, *55*, 23–39. [CrossRef] [PubMed]
5. Shafique, H.A.; Sultana, V.; Ehteshamul-Haque, S.; Athar, M. Management of soil-borne diseases of organic vegetables. *J. Plant Prot. Res.* **2016**, *56*, 221–230. [CrossRef]
6. Sharma, I.P.; Sharma, A. Physiological and biochemical changes in tomato cultivar PT-3 with dual inoculation of mycorrhiza and PGPR against root-knot nematode. *Symbiosis* **2017**, *71*, 175–183. [CrossRef]
7. Al-Hammouri, A.A.; Lindemann, W.; Thomas, S.; Sanogo, S. Effect of inoculum levels of *Rhizoctonia solani* and *Meloidogyne incognita* on chile pepper in soil simultaneously infested with both pathogens. *Res. Crop.* **2018**, *19*. [CrossRef]
8. Dean, R.; Van Kan, J.A.; Pretorius, Z.A.; Hammond-Kosack, K.E.; Di Pietro, A.; Spanu, P.D.; Rudd, J.J.; Dickman, M.; Kahmann, R.; Ellis, J. The Top 10 fungal pathogens in molecular plant pathology. *Mol. Plant Pathol.* **2012**, *13*, 414–430. [CrossRef]
9. Ozbay, N.; Newman, S.E. Fusarium crown and root rot of tomato and control methods. *Plant Pathol. J.* **2004**, *3*, 9–18.
10. Simbaqueba, J. Analysis of *Fusarium Oxysporum* Effectors Shared between Strains that Infect Cape Gooseberry and Tomato. Ph.D. Thesis, The Australian National University, Canberra, Australia, 2017.
11. Singh, V.K.; Singh, H.B.; Upadhyay, R.S. Role of fusaric acid in the development of 'Fusarium wilt'symptoms in tomato: Physiological, biochemical and proteomic perspectives. *Plant Physiol. Biochem.* **2017**, *118*, 320–332. [CrossRef]
12. Castagnone-Sereno, P.; Danchin, E.G.; Perfus-Barbeoch, L.; Abad, P. Diversity and evolution of root-knot nematodes, genus Meloidogyne: New insights from the genomic era. *Annu. Rev. Phytopathol.* **2013**, *51*, 203–220. [CrossRef]
13. Kyndt, T.; Vieira, P.; Gheysen, G.; de Almeida-Engler, J. Nematode feeding sites: Unique organs in plant roots. *Planta* **2013**, *238*, 807–818. [CrossRef] [PubMed]
14. Favery, B.; Quentin, M.; Jaubert-Possamai, S.; Abad, P. Gall-forming root-knot nematodes hijack key plant cellular functions to induce multinucleate and hypertrophied feeding cells. *J. Insect Physiol.* **2016**, *84*, 60–69. [CrossRef] [PubMed]
15. Grundler, F.M.; Hofmann, J. Water and nutrient transport in nematode feeding sites. In *Genomics and Molecular Genetics of Plant-Nematode Interactions*; Springer: Berlin, Germany, 2011; pp. 423–439.
16. Kassie, Y.G. Status of root knot nematode (*Meloidogyne* species) and fusarium wilt (*Fusarium oxysporum*) disease complex on tomato (*Solanum lycopersicum* L.) in the Central Rift Valley Ethopia. *Agri. Sci.* **2019**, *10*, 1090–1103.
17. Powell, N. Interaction of plant parasitic nematodes with other disease-causing agents. In *Plant Parasitic Nematodes*; Zuckerman, B.M., Mai, W.F., Rohde, R.A., Eds.; Academic Press: Cambridge, MA, USA, 2012; pp. 119–136.
18. Horrigue-Raouani, N. Variabilité de la relation hôte parasite dans le cas des *Meloidogyne* spp.(Nematoda: Meloidogynidae). Ph.D. Thesis, Université Tunis-El Manar, Faculté des Sciences de Tunis, Tunis, Tunisia, 2003.
19. Kazan, K.; Lyons, R. Intervention of phytohormone pathways by pathogen effectors. *Plant Cell* **2014**, *26*, 2285–2309. [CrossRef]

20. Hossain, Z.; Komatsu, S. Contribution of proteomic studies towards understanding plant heavy metal stress response. *Front. Plant Sci.* **2013**, *3*, 310. [CrossRef]
21. Li, C.; Zuo, C.; Deng, G.; Kuang, R.; Yang, Q.; Hu, C.; Sheng, O.; Zhang, S.; Ma, L.; Wei, Y. Contamination of bananas with beauvericin and fusaric acid produced by *Fusarium oxysporum* f. sp. cubense. *PLoS ONE* **2013**, *8*, e70226. [CrossRef]
22. Dias, J.S. Vegetable breeding for nutritional quality and health benefits. In *Cultivar: Chemical Properties, Antioxidant Activities and Health Benefits*; Nova Science Publishers Inc.: Hauppauge, NY, USA, 2012; pp. 1–81.
23. Palomares-Rius, J.E.; Castillo, P.; Trapero-Casas, J.L.; Jiménez-Díaz, R.M. Infection by *Meloidogyne javanica* does not breakdown resistance to the defoliating pathotype of *Verticillium dahliae* in selected clones of wild olive. *Sci. Hortic.* **2016**, *199*, 149–157. [CrossRef]
24. Abd-Elsalam, K.A.; Asran-Amal, A.; Schnieder, F.; Migheli, Q.; Verreet, J.A. Molecular detection of *Fusarium oxysporum* f. sp. *vasinfectum* in cotton roots by PCR and real-time PCR assay/Molekularer Nachweis von *Fusarium oxysporum* f. sp. *vasinfectum* in baumwolle mittels PCR und Real-Time-PCR. *J. Plant Dis. Prot.* **2006**, *113*, 14–19.
25. Koch, R. The aetiology of tuberculosis. *Berl. Klin. Wochenschr.* **1882**, *19*, 221–230.
26. Barker, K.; Hussey, R. Histopathology of nodular tissues of legumes infected with certain nematodes. *Phytopathology* **1976**, *66*, 851–855. [CrossRef]
27. Latif Khan, A.; Ahmed Halo, B.; Elyassi, A.; Ali, S.; Al-Hosni, K.; Hussain, J.; Al-Harrasi, A.; Lee, I.J. Indole acetic acid and ACC deaminase from endophytic bacteria improves the growth of *Solanum lycopersicum*. *Electron. J. Biotechnol.* **2016**, *19*, 58–64. [CrossRef]
28. Purwati, R.D.; Hidayah, N. Inoculation methods and conidial densities of *Fusarium oxysporum* f. sp. *cubense* in Abaca. *HAYATI J. Biosci.* **2008**, *15*, 1–7. [CrossRef]
29. Bybd, D., Jr.; Kirkpatrick, T.; Barker, K. An improved technique for clearing and staining plant tissues for detection of nematodes. *J. Nematol.* **1983**, *15*, 142–143. [PubMed]
30. Viglierchio, D.; Schmitt, R.V. On the methodology of nematode extraction from field samples: Baermann funnel modifications. *J. Nematol.* **1983**, *15*, 438–444. [PubMed]
31. Weydert, C.J.; Cullen, J.J. Measurement of superoxide dismutase, catalase and glutathione peroxidase in cultured cells and tissue. *Nat. Protoc.* **2010**, *5*, 51–56. [CrossRef]
32. Yong, Z.; Hao-Ru, T.; Ya, L. Variation in antioxidant enzyme activities of two strawberry cultivars with short-term low temperature stress. *World J. Agric. Sci.* **2008**, *4*, 458–462.
33. Cakmak, I.; Marschner, H. Magnesium deficiency and high light intensity enhance activities of superoxide dismutase, ascorbate peroxidase, and glutathione reductase in bean leaves. *Plant Physiol.* **1992**, *98*, 1222–1227. [CrossRef]
34. Esterbauer, H.; Schwarzl, E.; Hayn, M. A rapid assay for catechol oxidase and laccase using 2-nitro-5-thiobenzoic acid. *Anal. Biochem.* **1977**, *77*, 486–494. [CrossRef]
35. Li, F.; Ling, X.; Cao, X.; Wang, Z.; Shi, W.; Zhang, S. High specific monoclonal antibody production and development of an ELISA method for monitoring T-2 toxin in rice. *J. Agric. Food Chem.* **2014**, *62*, 1492–1497. [CrossRef]
36. Abbasi, H.; Akhtar, A.; Sharf, R. Vesicular arbuscular mycorrhizal (VAM) fungi: A tool for sustainable agriculture. *Am. J. Plant Nutr. Fertil. Technol.* **2015**, *5*, 40–49.
37. Kamran, M.; Malik, Z.; Parveen, A.; Huang, L.; Riaz, M.; Bashir, S.; Mustafa, A.; Abbasi, G.H.; Xue, B.; Ali, U. Ameliorative effects of biochar on rapeseed (*Brassica napus* L.) growth and heavy metal immobilization in soil irrigated with untreated wastewater. *J. Plant Growth Regul.* **2019**, 1–16. [CrossRef]
38. Arnon, D. Copper enzyme in isolated chloroplast and chlorophyll expressed in terms of mg per gram. *Plant Physiol.* **1949**, *24*, 1–15. [CrossRef] [PubMed]
39. Wellburn, A.R. The spectral determination of chlorophylls a and b, as well as total carotenoids, using various solvents with spectrophotometers of different resolution. *J. Plant Physiol.* **1994**, *144*, 307–313. [CrossRef]
40. Bates, L.S.; Waldren, R.P.; Teare, I. Rapid determination of free proline for water-stress studies. *Plant Soil* **1973**, *39*, 205–207. [CrossRef]
41. Dionisio-Sese, M.L.; Tobita, S. Antioxidant responses of rice seedlings to salinity stress. *Plant Sci.* **1998**, *135*, 1–9. [CrossRef]

42. Balestrini, R.; Cosgrove, D.J.; Bonfante, P. Differential location of α-expansin proteins during the accommodation of root cells to an arbuscular mycorrhizal fungus. *Planta* **2005**, *220*, 889–899. [CrossRef] [PubMed]
43. Pretty, J.; Toulmin, C.; Williams, S. Sustainable intensification in African agriculture. *Int. J. Agric. Sustain.* **2011**, *9*, 5–24. [CrossRef]
44. Dracatos, P.M.; Haghdoust, R.; Singh, D.; Park, R.F. Exploring and exploiting the boundaries of host specificity using the cereal rust and mildew models. *New Phytol.* **2018**, *218*, 453–462. [CrossRef]
45. Ramalingam, K. Exploring the disease severity by the interaction of fusarium wilt and root knot nematode in tomato. *Int. J. Fauna Biol. Stud.* **2019**, *6*, 1–5.
46. Al-Hazmi, A.; Al-Nadary, S. Interaction between *Meloidogyne incognita* and *Rhizoctonia solani* on green beans. *Saudi J. Biol. Sci.* **2015**, *22*, 570–574. [CrossRef]
47. Saeedizadeh, A.; Kheiri, A.; Okhovat, M.; Hoseininejad, A. Study on interaction between root-knot nematode *Meloidogyne javanica* and wilt fungus *Verticillium dahliae* on olive seedlings in greenhouse. *Commun. Agric. Appl. Biol. Sci.* **2003**, *68*, 139–143. [PubMed]
48. Mallaiah, B.; Muthamilan, M.; Prabhu, S.; Ananthan, R. Studies on interaction of nematode, *Pratylenchus delattrei* and fungal pathogen, *Fusarium incarnatum* associated with crossandra wilt in Tamil Nadu, India. *Curr. Biot.* **2014**, *8*, 157–164.
49. Hua, G.K.H.; Timper, P.; Ji, P. *Meloidogyne incognita* intensifies the severity of fusarium wilt on watermelon caused by *Fusarium oxysporum* f. sp. *niveum*. *Can. J. Plant Pathol.* **2019**, *41*, 261–269. [CrossRef]
50. Mai, W.; Abawi, G. Interactions among root-knot nematodes and Fusarium wilt fungi on host plants. *Annu. Rev. Phytopathol.* **1987**, *25*, 317–338. [CrossRef]
51. Manzanilla-López, R.H.; Esteves, I.; Devonshire, J. Biology and management of Pochonia chlamydosporia and plant-parasitic nematodes. In *Perspectives in Sustainable Nematode Management through Pochonia Chlamydosporia Applications for Root and Rhizosphere Health*; Springer: Berlin, Germany, 2017; pp. 47–76.
52. Pshibytko, N.; Zenevich, L.; Kabashnikova, L. Changes in the photosynthetic apparatus during Fusarium wilt of tomato. *Russian J. Plant Physiol.* **2006**, *53*, 25–31. [CrossRef]
53. Verbančič, J.; Lunn, J.E.; Stitt, M.; Persson, S. Carbon supply and the regulation of cell wall synthesis. *Mol. Plant* **2018**, *11*, 75–94. [CrossRef]
54. Voiniciuc, C.; Pauly, M.; Usadel, B. Monitoring polysaccharide dynamics in the plant cell wall. *Plant Physiol.* **2018**, *176*, 2590–2600. [CrossRef]
55. Bleve-Zacheo, T.; Melillo, M.T.; Castagnone-Sereno, P. The contribution of biotechnology to root-knot nematode control in tomato plants. *Pest Technol.* **2007**, *1*, 1–16.
56. Pask, A.; Pietragalla, J.; Mullan, D.; Reynolds, M. *Physiological Breeding II: A Field Guide to Wheat Phenotyping*; CIMMYT: El Batán, Texcoco, Mexico, 2012.
57. Stoeva, N.; Bineva, T. Oxidative changes and photosynthesis in oat plants grown in As-contaminated soil. *Bulg. J. Plant Physiol.* **2003**, *29*, 87–95.
58. de Oliveira Silva, F.M.; Lichtenstein, G.; Alseekh, S.; Rosado-Souza, L.; Conte, M.; Suguiyama, V.F.; Lira, B.S.; Fanourakis, D.; Usadel, B.; Bhering, L.L. The genetic architecture of photosynthesis and plant growth-related traits in tomato. *Plant Cell Environ.* **2018**, *41*, 327–341. [CrossRef]
59. Ort, D.R.; Merchant, S.S.; Alric, J.; Barkan, A.; Blankenship, R.E.; Bock, R.; Croce, R.; Hanson, M.R.; Hibberd, J.M.; Long, S.P. Redesigning photosynthesis to sustainably meet global food and bioenergy demand. *Proc. Natl. Acad. Sci. USA* **2015**, *112*, 8529–8536. [CrossRef] [PubMed]
60. Barna, B.; Ádám, A.; Király, Z. Juvenility and resistance of a superoxide tolerant plant to diseases and other stresses. *Naturwissenschaften* **1993**, *80*, 420–422. [CrossRef]
61. Bakhat, H.F.; Bibi, N.; Zia, Z.; Abbas, S.; Hammad, H.M.; Fahad, S.; Ashraf, M.R.; Shah, G.M.; Rabbani, F.; Saeed, S. Silicon mitigates biotic stresses in crop plants: A review. *Crop Prot.* **2018**, *104*, 21–34. [CrossRef]
62. Zhao, X.; Zhen, W.; Qi, Y.; Liu, X.; Yin, B. Coordinated effects of root autotoxic substances and Fusarium oxysporum Schl. f. sp. fragariae on the growth and replant disease of strawberry. *Front. Agric. China* **2009**, *3*, 34. [CrossRef]
63. Lu, P.; Davis, R.F.; Kemerait, R.C.; van Iersel, M.W.; Scherm, H. Physiological effects of *Meloidogyne incognita* infection on cotton genotypes with differing levels of resistance in the greenhouse. *J. Nematol.* **2014**, *46*, 352–359. [PubMed]

64. Sharma, P.; Jha, A.B.; Dubey, R.S.; Pessarakli, M. Reactive oxygen species, oxidative damage, and antioxidative defense mechanism in plants under stressful conditions. *J. Bot.* **2012**, *2012*. [CrossRef]
65. Zhou, R.; Yu, X.; Ottosen, C.O.; Rosenqvist, E.; Zhao, L.; Wang, Y.; Yu, W.; Zhao, T.; Wu, Z. Drought stress had a predominant effect over heat stress on three tomato cultivars subjected to combined stress. *BMC Plant Biol.* **2017**, *17*, 24. [CrossRef]
66. Sharf, R.; Hisamuddin, A.; Akhtar, A. Management of root-knot disease in *Phaseolus vulgaris* using potassium fertilizer and biocontrol agents. *J. Plant Pathol. Microbiol.* **2014**, *5*, 1.
67. Barker, K.; Olthof, T.H. Relationships between nematode population densities and crop responses. *Annu. Rev. Phytopathol.* **1976**, *14*, 327–353. [CrossRef]
68. Meena, K.S.; Ramyabharathi, S.; Raguchander, T.; Jonathan, E. Interaction of *Meloidogyne incognita* and *Fusarium oxysporum* in carnation and physiological changes induced in plants due to the interaction. *SAARC J. Agric.* **2016**, *14*, 59–69. [CrossRef]
69. Jones, H. Partitioning stomatal and non-stomatal limitations to photosynthesis. *Plant Cell Environ.* **1985**, *8*, 95–104. [CrossRef]
70. Gomes, V.M.; Souza, R.M.; Midorikawa, G.; Miller, R.; Almeida, A.M. Guava Decline: Evidence of Nationwide Incidence in Brazil [deterioro del guayabo: Evidencia de la incidencia en brasil]. *Nematropica* **2012**, *42*, 153–162.
71. Allahverdiyeva, Y.; Aro, E.-M. Photosynthetic responses of plants to excess light: Mechanisms and conditions for photoinhibition, excess energy dissipation and repair. In *Photosynthesis*; Springer: Berlin, Germany, 2012; pp. 275–297.
72. Yu, J.; Zhang, Y.; Liu, J.; Wang, L.; Liu, P.; Yin, Z.; Guo, S.; Ma, J.; Lu, Z.; Wang, T. Proteomic discovery of H_2O_2 response in roots and functional characterization of PutGLP gene from alkaligrass. *Planta* **2018**, *248*, 1079–1099. [CrossRef] [PubMed]
73. Gill, S.S.; Tuteja, N. Reactive oxygen species and antioxidant machinery in abiotic stress tolerance in crop plants. *Plant Physiol. Biochem.* **2010**, *48*, 909–930. [CrossRef] [PubMed]
74. Kesba, H.H.; El-Beltagi, H.S. Biochemical changes in grape rootstocks resulted from humic acid treatments in relation to nematode infection. *Asian Pac. J. Trop. Biomed.* **2012**, *2*, 287–293. [CrossRef]
75. Shoresh, M.; Harman, G.E.; Mastouri, F. Induced systemic resistance and plant responses to fungal biocontrol agents. *Annu. Rev. Phytopathol.* **2010**, *48*, 21–43. [CrossRef]
76. Ma, X.; Zhang, X.; Yang, L.; Tang, M.; Wang, K.; Wang, L.; Bai, L.; Song, C. Hydrogen peroxide plays an important role in PERK4-mediated abscisic acid-regulated root growth in Arabidopsis. *Funct. Plant Biol.* **2019**, *46*, 165–174. [CrossRef]
77. Molinari, S.; Fanelli, E.; Leonetti, P. Expression of tomato salicylic acid (SA)-responsive pathogenesis-related genes in Mi-1-mediated and SA-induced resistance to root-knot nematodes. *Mol. Plant Pathol.* **2014**, *15*, 255–264. [CrossRef]
78. Eissa, M.F.; Abd-Elgawad, M.M. Nematophagous bacteria as biocontrol agents of phytonematodes. In *Biocontrol Agents of Phytonematodes*; CAB International: Wallingford, UK, 2015; pp. 217–243.
79. Arora, A.; Sairam, R.; Srivastava, G. Oxidative stress and antioxidative system in plants. *Curr. Sci.* **2002**, *82*, 1227–1238.
80. Quan, L.J.; Zhang, B.; Shi, W.W.; Li, H.Y. Hydrogen peroxide in plants: A versatile molecule of the reactive oxygen species network. *J. Integr. Plant Biol.* **2008**, *50*, 2–18. [CrossRef]
81. Woin, N.; Tata Ngome, P.; Waingeh, N.; Adjoudji, O.; Nossi, E.; Simo, B.; Yingchia, Y.; Nsongang, A.; Adama, F.; Mveme, M. *Suitability of Different Processing Techniques and Sales Options for Irish Potato (Solanum Tuberusum) Cultivars in Cameroon*; FARA Research Report: Accra, Ghana, 2019; pp. 2550–3359.
82. Awan, Z.A.; Shoaib, A.; Khan, K.A. Variations in total phenolics and antioxidant enzymes cause phenotypic variability and differential resistant response in tomato genotypes against early blight disease. *Sci. Hortic.* **2018**, *239*, 216–223. [CrossRef]
83. Arshad, W.; Waheed, M.T.; Mysore, K.S.; Mirza, B. Agrobacterium-mediated transformation of tomato with rolB gene results in enhancement of fruit quality and foliar resistance against fungal pathogens. *PLoS ONE* **2014**, *9*, e96979. [CrossRef] [PubMed]
84. Hlatshwayo, S.G. Involvement of abscisic acid and H_2O_2 in antioxidant enzyme activities mediated by nitric oxide synthase-like activity in maize. Ph.D. Thesis, University of the Western Cape, Cape Town, South Africa, 2018.

85. Yang, Y.X.; Ahammed, G.J.; Wu, C.; Yang, Z.; Wan, C.; Chen, J. Red light-induced systemic resistance against root-knot nematode is mediated by a coordinated regulation of salicylic acid, jasmonic acid and redox signaling in watermelon. *Front. Plant Sci.* **2018**, *9*, 899. [CrossRef] [PubMed]
86. McGovern, R. Management of tomato diseases caused by *Fusarium oxysporum*. *Crop Prot.* **2015**, *73*, 78–92. [CrossRef]